enanonewsletter
Special Issue /// December 2011 www.phantomsnet.net

Graphene Position Paper
(nanoICT Working Group)

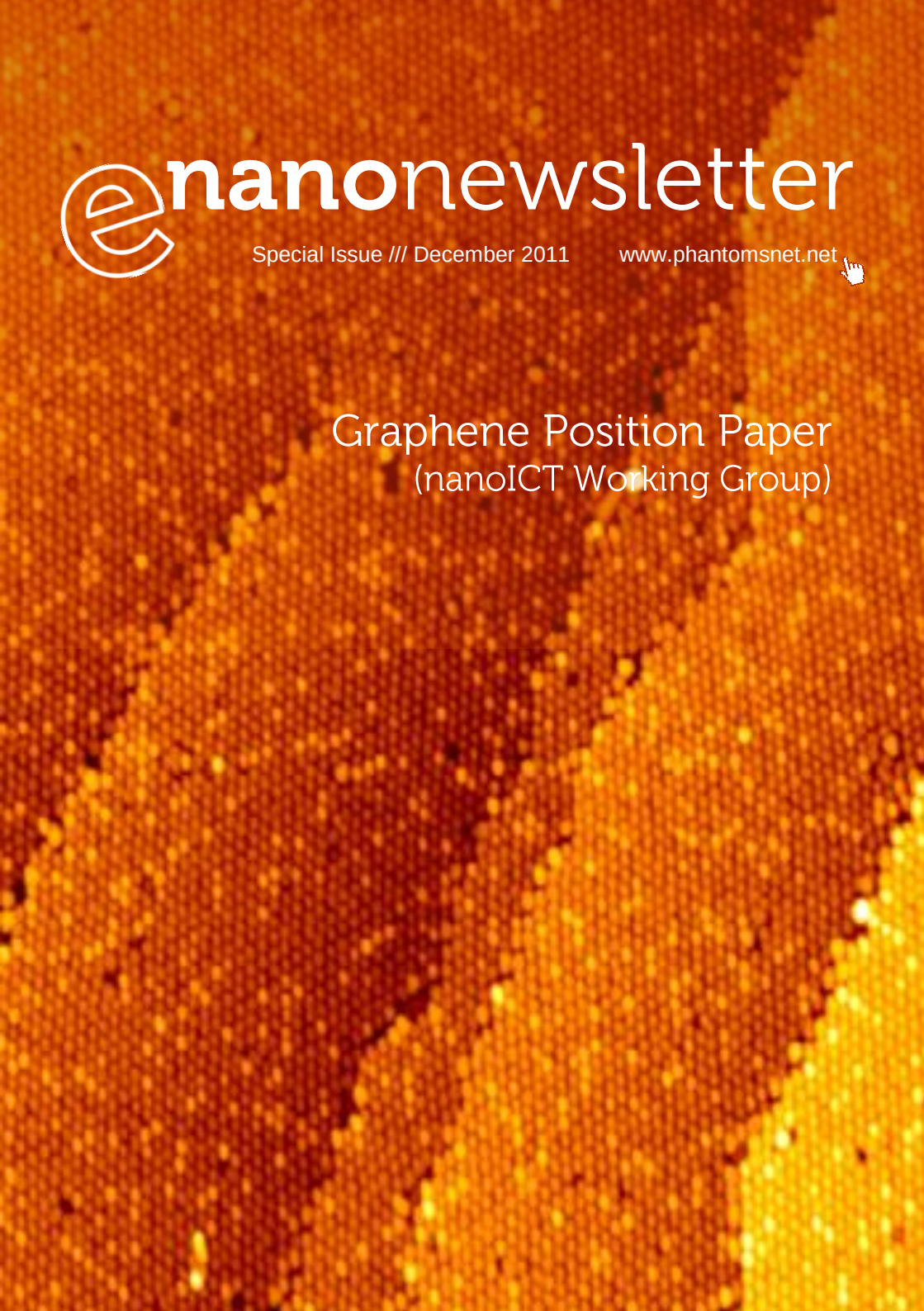

graphene 2012

April 10-13, 2012
Brussels (Belgium)
www.graphene2012.com

graphene
International Conference

Graphene Flagship Session

The consortium of the Graphene Flagship Pilot Action is working to establish the "Graphene Science and Technology Roadmap" which will be presented to the European Commission and Member States to demonstrate the need for securing long term funding, coordinated through a new Graphene Alliance. The Graphene Flagship Pilot Action will take advantage of the International conference Graphene2012 in Brussels to co-organize a specific session in order to timely deliver to the European community the results of this Roadmap.

PHANTOMS foundation

UCL Université catholique de Louvain

ICN2 Institut Català de Nanotecnologia

cnrs

dear readers,

This E-nano Newsletter special issue contains the final version of the nanoICT position paper on Graphene (one-atom-thick sheet of carbon / in 2010, A.K. Geim and K. Novoselov, were awarded the Nobel Prize in physics for “groundbreaking experiments regarding the two-dimensional material graphene”) summarising the current state of progress and open perspectives concerning the emergence of graphene-based technologies and applications. This paper is a mixture between a short review of recent achievements and ingredients for the elaboration of a more specific and detailed roadmap.

In that direction, one should mention the initiative named GRAPHENE FLAGSHIP pilot action (see www.graphene-flagship.eu) which principal objective is to bring together a focused, interdisciplinary European research community that aims at a radical technology shift in information and communication technology that exploits the unique properties of graphene and related two-dimensional materials.

I hope you will enjoy reading this document.

We would like to thank all the authors who contributed to this issue as well as the European Commission for the financial support (project nanoICT No. 216165).

> **Dr. Antonio Correia** Editor - Phantoms Foundation

contents

editorial information

Special Issue. December 2011. Published by Phantoms Foundation (Spain)

editor > Dr. Antonio Correia > **antonio@phantomsnet.net**

assistant editors > Carmen Chacón, Viviana Estêvão, Maite Fernández, Conchi Narros and José Luis Roldán.

1500 copies of this issue have been printed. Full color newsletter available at: **www.phantomsnet.net/Foundation/newsletter.php**

For any question please contact the editor at: **antonio@phantomsnet.net**

depósito legal / legal deposit
BI-2194/2011

printing
Gráficas Valdés, S.L.

foreword

Within Nano-ICT coordinated action, a GRAPHENE Working Group (GWG) was established with the aim of gathering European scientists involved in graphene research, to highlight the latest developments in graphene material growth, characterization and devices, identifying the technological bottlenecks and challenges, and brainstorming solutions to take these technologies from lab to industry. Two meeting were celebrated during GRAPHENE 2011 in Bilbao and TNT2011 in Tenerife.

Although the discovery of graphene and most of its peculiar physical properties has been achieved in Europe, international competition has become fierce, especially in boosting technological innovation in a broad spectrum of applications (flexible electronics, photonics, energy, sensors, functional composites, and so forth). To overcome fragmentation issues and establish a long term program for science and technology innovation, European researchers have been networked through the GRAPHENE FLAGSHIP pilot action (www.graphene-flagship.eu) coordinated by Chalmers University and which has attracted a considerable interest with more than 500 groups thousands of researchers registered to the web database. Based on genuine synergies with scientific communities of members states including Spain (through the *Spanish mobilizing action*, see www.icmm.csic.es/graphene/), France and Belgium (through the *GDR Graphene and nanotubes* network, see www.graphene-nanotubes.org), Germany or Netherlands (FOM program, see www.graphene.nl) to cite a few, the Graphene Flagship is preparing the **European graphene roadmap for Science and Technology innovation**, to be delivered during GRAPHENE 2012 in Brussels in April 2012 (www.graphene2012.com).

The position paper presented afterwards can be seen as a compacted view of the state of graphene research in Europe and overseas, while giving some flavor of road-mapping, pinpointing several directions of important challenges for European researchers.

The content of the position paper includes overview of large scale catalytic growth, exfoliation and wafer bonding approaches of graphene monolayers and few layers compounds, integration with other materials (nanotubes, organics, metals and semiconductors, defect characterization and defect engineering (doping, functionalization, patterning, indentation), nanoelectronics (field effect transistors), RF-applications (THz), magnetism and Spintronics, electro-mechanical devices, optical properties, nanophotonics, as well as theoretical properties, and device simulation.

> **Dr. Stephan Roche**
ICREA Research Professor, Catalan Institute of Nanotechnology (Spain)

nanoresearch

Graphene position paper

Francesco Bonaccorso> University of Cambridge, UK
Johann Coraux> Néel Institute, France
Chris Ewels>IMN Nantes, France
Gianluca Fiori> University of Pisa, Italy
Andrea C. Ferrari> University of Cambridge, UK
Jean-Christophe Gabriel> CEA, INAC, France
Mar Garcia-Hernandez> ICMM CSIC, Spain
Jari Kinaret> Chalmers University of Technology, Sweden
Max Lemme> KITH, Sweden
Daniel Neumaier> AMO, Germany
Vincenzo Palermo> CNR Bologna, Italy
Aziz Zenasni> CEA, LETI, France
Stephan Roche> Catalan Institute of Nanotechnology and ICREA, Spain

Key Words

Growth: *CVD growth, epitaxial growth, modelling.*
Post-growth modification: *Doping, & functionalization, dispersion and separation, purification, annealing.*
Properties/characterization: *Defects, electron transport, phonons, thermal properties/conductivity, wetting, friction, mechanical, chemical properties, optical, structural properties, contacts.*
Electronic Applications: *RF devices, transistors, sensors, touch screens, flat displays, flexible electronics.*
Optical applications: *OLED, Absorbers, photodetectors, photovoltaics...*
Electromechanical applications: *NEMS (resonators), sensors, bio-medical.*
Energy applications: *Fuel cells, supercapacitors, batteries, solar cells.*
Blue sky: *Spintronics, quantum computing, plasmonics.*

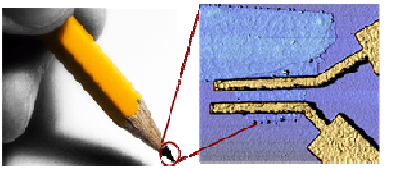

Introduction

In this paper, we aim to position the current state and perspectives of graphene-based technologies and applications. This is not meant to be a comprehensive review of the field, but rather an overview with particular focus on European strengths and potential. Non-European researchers clearly give a huge contribution to the field, and set the benchmark against which the European work is measured.

7 years ago, the ground-breaking experiments on graphene in Manchester initiated a field of research moving at an ever faster rate, and gained the 2010 Physics Nobel prize to Andre Geim and Kostya Novoselov.

Even though, graphene science and technology has been pioneered in Europe, international competition is and will remain fierce, given the extensive applications domain. Graphene and related two-dimensional materials offer a completely new *"flatland playground"* for physicists, chemists and engineers. After the discovery of fullerene and carbon nanotubes, graphene has complemented the sp^2 carbon family, being at the same time more suitable for (co)-integration and connection to CMOS technologies, benefiting from conventional techniques of lithography and material engineering. Graphene also appears as a unique platform bridging conventional technologies with the nanoscale Pandora´s box, enabling chemistry to enrich material and device properties.

Graphene-based materials as thus "*enabling materials for ubiquitous electronics applications*" in the fields of information and communication technology (ICT), energy or medicine/biology. Beyond Graphene and the (two-dimensional) flatland, engineering novel materials using the third dimension is also matter of excitement and future innovation. During his Plenary talk at IMAGINENANO 2011

(Bilbao April 2011, www.imaginenano.com), Kostya Novoselov called the scientific community to explore the "spaceland" which could complement graphene through its combination with other two-dimensional exfoliated materials (such as Boron-Nitride)[1]. This opens unprecedented horizons for the design of materials on demand, supplying the suitable structure for a given properties portfolio. Europe could take an international leadership in "novel material innovation", provided a strategic scientific and industrial roadmapping, implementation plan, team networking and relevant funding are smartly merged.

We report here a summary of recent developments in graphene science and technology, pinpointing future directions for innovation and discovery, with a particular emphasis on positioning the prospects for European research. This first version of the Nano-ICT position paper is thus to be considered a mixture between a short review of recent achievements and ingredients for the elaboration of a more specific and detailed roadmap, and not a comprehensive and final review and roadmapping exercise.

In that direction, a particular mention deserves the initiative named GRAPHENE FLAGSHIP pilot (see www.graphene-flagship.eu) which is currently establishing a large database of European groups and research activities focused on Graphene Science and Applications. To date more than 500 groups have registered, gathering several thousands of researchers and engineers and more than thirty companies. This initiative will issue a more exhaustive graphene roadmap in 2012.

Vision for the future

A.K.Geim and K. Novoselov, were awarded the 2010 Nobel Prize in physics for "*groundbreaking experiments regarding the two-dimensional material graphene*". Graphene is a one-atom-thick sheet of carbon whose strength, flexibility, and electrical conductivity have opened new horizons for fundamental physics, together with technological innovations in electronic, optical, and energy sectors.

The production of high quality graphene remains one of the greatest challenges, in particular when it comes to maintaining the material properties and performance upon up-scaling, which includes mass production for material/energy-oriented applications and wafer-scale integration for device/ICTs-oriented applications (see Fig.1 for illustration).

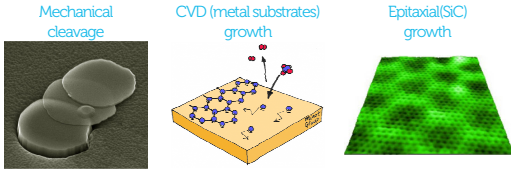

Fig. 1 > Illustration of various techniques to either separate out a graphene monolayer by mechanical/chemical exfoliation of layers from graphite, CVD grow graphene on a metallic substrate, or epitaxial growth of graphene layers at the surface of Silicon Carbide./

Potential electronics applications of graphene include high-frequency devices and RF communications, touch screens, flexible and wearable electronics, as well as ultrasensitive sensors, NEMS, super-dense data storage, or photonic devices (see Fig.2). In the energy field, potential applications include supercapacitors to store and transit electrical power, and highly efficient solar cells. However, in the medium term, some of graphene's most appealing potential lies in its ability to transmit light as well as electricity, offering improved performances of light emitting diodes (LEDs) and aid in the production of next-generation devices like flexible touch screens, photodetectors, and ultrafast lasers.

There are many other potential uses of graphene because of its unique combination of properties. Graphene is transparent like plastic but conducts heat and electricity better than metal, it is an

elastic thin film, behaves as an impermeable membrane, and it is chemically inert and stable. In 2010 Ref [2] reported the first roll-to-roll production and wet-chemical doping of predominantly monolayer 30-inch graphene films grown by chemical vapour deposition (CVD) onto flexible copper substrates. The produced films were characterized by low sheet resistances (Rs) and 90% transmittance (T), competing with commercial transparent electrodes such as indium tin oxides (ITO). This work demonstrated that graphene electrodes can be efficiently incorporated into a fully functional touch-screen capable of withstanding high strain. Such results allow us to envision the development of a revolutionary flexible, portable and reconfigurable electronics, as pioneered by NOKIA through the MORPH concept (See Fig.3).

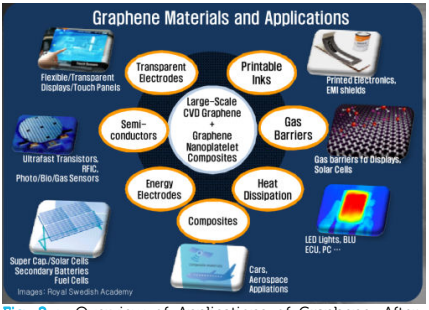

Fig. 2 > Overview of Applications of Graphene. After Royal Swedish academy [3]. (by courtesy of Byung Hee Hong Seoul National). /

New horizons have also been opened from the demonstration of high-speed graphene circuits [4] offering high-bandwidth suitable for the next generation of low-cost smart phone and television displays.

Concerning the domain of ICT, CMOS technology, as currently used in integrated circuits, is rapidly approaching the limits of downsizing transistors, and graphene is seen as an alternative. However, the technology to produce graphene circuits is still in its infancy, and probably at least a decade of additional effort will be necessary, for example to avoid costly transfer from metal substrates. The device yield rate also needs to be improved.

The use of graphene in electrodes is probably the closest to commercialization.

Fig. 3 > Graphene in NOKIA Morph concept: the future mobile device, Morph, will act as a gateway. It will connect users to the local environment as well as the global internet. It is an attentive device that shapes according to the context. The device can change its form from rigid to flexible and stretchable. For more information see [5]. /

In 2011 Ref. [4] reported the first wafer-scale graphene circuit (broadband frequency mixer) in which all circuit components, including graphene field-effect transistors (FETs) and inductors, were monolithically integrated on a single carbide wafer. The integrated circuit operated as a broadband radio-frequency mixer at frequencies up to 10GHz, with outstanding thermal stability and little reduction in performance (less than one decibel) between 300 and 400K.

These results pave the way to achieving practical graphene technology with more complex functionality and performance.

Another potential field of application is photonics and optoelectronics, where the combination of its unique optical and electronic properties can be fully exploited, even in the absence of a band-gap, and the linear dispersion of the Dirac electrons enables ultrawideband tunability. The rise of graphene in photonics and optoelectronics is shown by several recent results, ranging from solar cells and light-emitting devices to touch screens, photodetectors and ultrafast lasers.

Graphene is promising as addictive for composite materials, thin films and conducting inks. High quality graphene inks [6] can now be produced via solution processing [7] and ink-jet printed thin film transistors with mobility ~90cm^2/Vs have already been demonstrated, paving the way towards fully graphene-based printable electronics [6].

Scientific output

Europe is competitively placed in terms of scientific output, with total graphene publications[1] from North America and Europe closely matching (see Fig. 4).

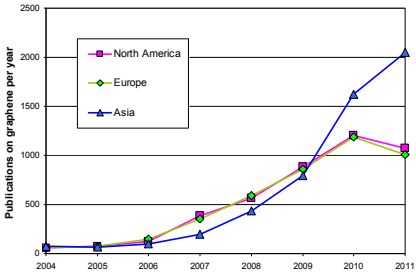

Fig. 4 > Total scientific publications on graphene by region (2011 January-September)./

The rise in output from Asia since 2009 is clear, largely due to a rapid increase from China, in 2011 overtaking the US as the largest producer of graphene publications. While the division in academic graphene publications between Europe, North America and Asia is roughly equal (Fig.5(left)), the US produced so far over three times as many patents as the others (Fig.5(right)), with the ten highest applicants for patents[2] divided between US academia (Rice University, MIT, University of California and Harvard) and US industry (Sandisk 3D, Graftech, Hyperion Catalysis International,General Electric and BASF)[8]. This, to some extent, reflects the different patent regimes in the regions, and Europe is once again well placed with nearly twice as many patent applications as Asia. The importance placed on graphene research by Korea, Japan and Singapore is clearly represented in their patent and publication output. Within Europe the majority of scientific publications comes from Germany, the UK and France (followed closely by Spain and Italy), while European patent activity is concentrated in Germany and the UK (see Fig.6).

[1] Topic search on 'graphene' from Thomson ISI Web of Science database. Note that this does not take into account any additional criteria such as impact factor of the publishing journals.

[2] Patent search on 'graphene' from the WIPO Patentscope international patent application database.

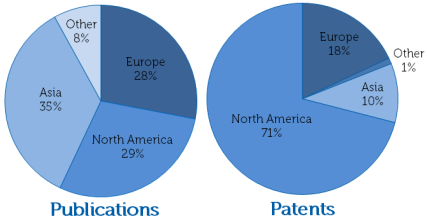

Fig. 5 > (Left) Total scientific publications and (Right) total patents on graphene by region. Source: Publications from Thomson ISI Web of Science 'graphene' topic search, Patents from WIPO PATENTSCOPE international patent applications./

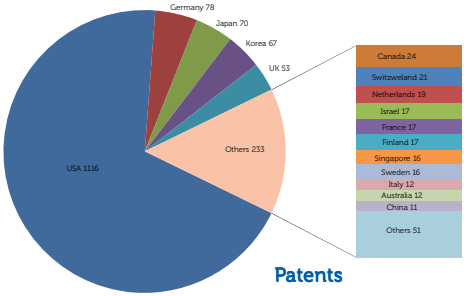

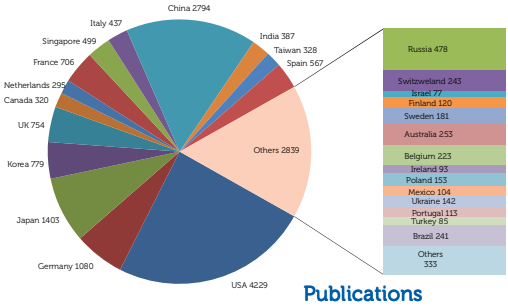

Fig. 6 > Breakdown of total patents and publications on graphene by country. Source: Publications from Thomson ISI Web of Science 'graphene' topic search; Patents from WIPO PATENTSCOPE international patent applications./

The sp^2 two-dimensional lattice: essentials

Graphene consists of carbon atoms arranged in a 2-dimensional honeycomb crystal lattice with a bond length of 1.42 Å [9,10]. A schematic of a single layer graphene (SLG) is shown in Fig. 7a, including "armchair" and "zig-zag" edges, named after their characteristic appearance on the atomic scale. The carbon atoms are sp^2 hybridized and three of the four valence electrons participate in the bonds to their next neighbours (σ–bonds). The schematic in Fig. 7b shows these in green (colour online). The fourth π electron orbital is oriented perpendicular to the sheet, forming with the neighbouring ones a highly delocalized network of π bonds (Fig. 7b, red).

The graphene lattice consists of two sub-lattices A and B, which lead to crystal symmetry [11,12]. As a consequence, the charge carriers (*n*) can be described by the Dirac equation [12], *i.e.* the band structure of graphene exhibits a linear dispersion relation for n, with momentum k proportional to energy E [12]. The energy bands associated with the sublattices intersect at zero energy. For this configuration graphene has been "commonly" called a zero bang gap semiconductor. However, the conductivity of graphene is independent of the Fermi energy (E_F) and n as long as the dependence of scattering strength on E_F and n is neglected [13].Thus graphene should be considered a metal rather than a semiconductor [13].

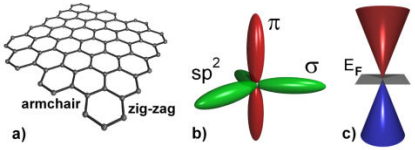

Fig. 7 > a) Schematic of a graphene crystallite with characteristic armchair and zig-zag edges. b) Schematic of electron σ–bonds and π-electron orbitalof one carbon atom in graphene. c) Band diagram of graphene at k = 0; From [14]./

A schematic of the band structure close to k = 0 including the Fermi level, E_F, is shown in Fig. 7c.

Charge carriers in graphene have a very small effective mass [15], hence graphene shows extremely attractive properties relevant to electronic devices. These include carrier mobilities of up to 15000 cm^2/Vs for graphene on SiO_2 [15], 27000 cm^2/Vs for epitaxial graphene [16] and hundreds of thousands of cm^2/Vs for suspended graphene [17,18,19] (Fig. 8), for typical charge density (n) ~$10^{12}cm^{-2}$. Very recently, mobilities up to 10^6 cm^2/Vs with n of $10^{11}cm^{-2}$ were reported for suspended graphene at helium liquid temperature [20]. These mobility values are at least 40 times higher than typical Si mobility. In addition, high current carrying capability exceeding 1x10^8 A/cm^2 [21], high thermal conductivity [22,23], high transparency [24] and mechanical stability [25,26] have been reported. While similar promising properties have been reported for carbon nanotubes (CNTs)[27], the fact that graphene processing is compatible with conventional CMOS-technology is potentially a huge advantage.

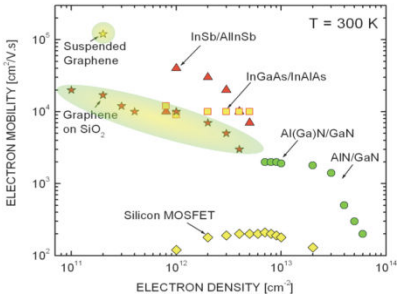

Fig. 8 >Electron mobility versus density for an ensemble of materials, positioning graphene performances. Extracted from [17,18,19]./

Graphene chemistry: not a molecule, not a polymer, not a substrate

Graphene chemical properties have raised great interest and stimulated excellent research. The main reason of interest is that graphene cannot be easily classified from a chemical point of view, having a size which is atomic in one dimension, and mesoscopic in the other two, resulting particular and somehow contrasting properties.

Graphene can be patterned, etched and coated as a substrate. It can also be processed in solution and chemically functionalized, as a molecule. It could be considered a polymer, obtained by bottom-up assembly of smaller molecules [28], but it can also be obtained from top-down exfoliation of graphite (a mineral). It is not a nano-object similar to fullerenes or CNTs, because it does not have a well-defined shape; conversely, it is a large, highly anisotropic, very flexible ultra-thin material, which can have different shapes and be folded, rolled or bent.

The simplest and most studied chemical functionalization of graphite is oxidation [29,30,31]. This leads to the production of graphene oxide (GO), [29,30,31], with the formation of defects such as C-OH, COOH and C-O-C bridges on its surface and at edges. The functionalization with these hydrophilic groups greatly favours GO exfoliation, allowing to produce on large scale highly concentrated solutions of GO in water [32], containing high percentage of monolayers [33].

The chemical polar groups created by oxidation can also be used for further functionalization, allowing to exploit the full power of carbon-based organic synthesis to achieve different graphene-based materials (Fig. 9a) [34,35]. By taking advantage of the extensive know-how already available for CNTs, either covalent [36,37] or supramolecular [38,39] functionalization of graphene with different molecules can be achieved. This includes selective organic functionalization of graphene edges, taking advantage of the higher concentration of carboxyilic groups at the edges of exfoliated GO sheets [34].

Chemical functionalization from one hand makes graphene more processable, but from the other hand destroys its peculiar electronic properties, transforming it into an insulator [40]. The GO chemical structure can be highly variable, depending on the details of its production, but can be described as a mosaic of different domains, of nanometer size, featuring highly conjugated, graphene-like areas, alternated to completely oxidized, insulating sp^3 domains, as well as to void areas where the oxidation process has completely destroyed the carbon backbone, leaving a hole in the GO sheet [41,42]. Overall, the surviving graphene conjugated domains in GO can be seen as an ensemble of polycyclic aromatic domains of different size, all linked on the same sheet by a network of insulating sp^3 bonds, which hinder charge transport [42].

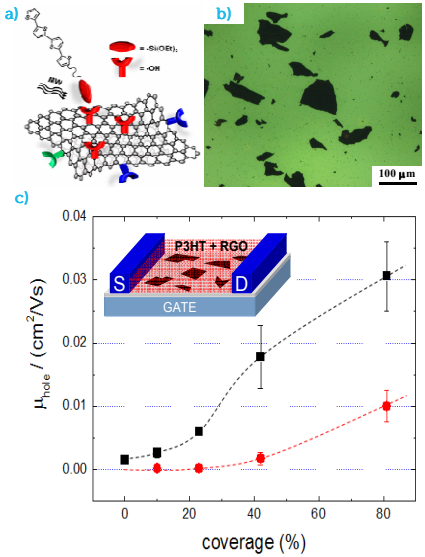

Fig. 9> a) Schematic representation of covalent functionalization of GO. From [35] b) Fluorescence quenching image of graphene oxide sheets on a thin molecular layer of quater-thiophene. From [43] c) Evolution of measured charge mobility in transistor devices based on polythiophene (P3HT) and reduced graphene oxide (RGO) at increasing RGO coverage. In the inset, a schematic representation of the transistor device. From [35]./

The conductivity can be increased by producing Reduced Graphene Oxide (RGO). Reduction can be achieved by thermal [40,55,44] chemical [40,45,46] or electrochemical [47,48] methods. Though this process never re-establishes the "perfect" lattice of graphene, being unable to heal some more stable defects, such as the voids in the sheets and some particular oxidized forms (carbonyl and ether groups) [49]. Nonetheless, RGO is conductive, with a

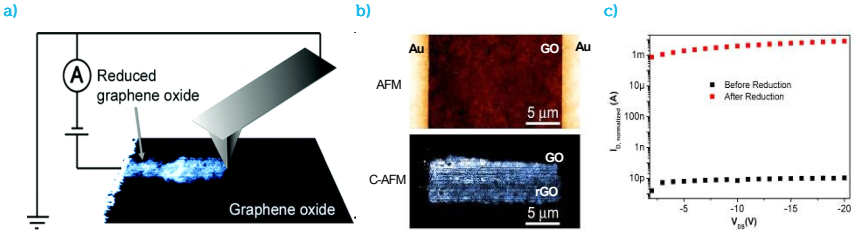

Fig. 10 > a) Schematic representation of the creation of conducting RGO patterns on an insulating GO layer using a scanning probe. b) AFM and conductive AFM image of a source-drain electrode pair bridged by an electrically conducting tip-reduced GO region. c) Drain current (I_D) vs. drain-source voltage (V_{DS}) measured on graphite oxide films before (black squares) and after (red squares) reduction by a scanning probe. An increase of about 10^8 in the normalized source-drain current is shown. From [57]./

charge mobility larger than typical organic semiconductors, and can have promising applications as electrode [50] and charge transporter [33,51] in organic electronics, as interface layer in photovoltaic blends [52], to replace or improve indium tin oxide (ITO) electrodes, in dye sensitized solar cells, to improve charge collection and transport [53] and as material with high surface area and good conductivity for energy storage [54].

An approach for selective GO reduction is to use a scanning probe by locally applying high temperature [55], or to perform electrochemical reduction on microscopic scale [56], allowing to fabricate electronic devices where the active layer is formed by a sheet of conductive RGO "drawn" on an otherwise insulating GO layer (Fig. 10a) [57]. Once functionalized, either by covalent or supramolecular chemistry, graphene interacts strongly with the surrounding molecules (either small molecules or polymers), gaining new electronic, chemical and optical properties. Graphene-organic interactions are studied for a wide range of applications, form surface science [39], to electronics [33,54,56] to composites, to biological and sensing applications [58,59,60].

Organic molecules can be absorbed on graphene substrates forming 2D layers which tend to have a weak interaction with the underlying graphene [39], with small but significant differences with respect to the packing of the same molecules on bulk graphite [39]. The graphene-molecule interaction can be strong, resulting in a complex interplay of π-π stacking, electrostatic interactions, and molecule-molecule lateral interactions [39,61,62].

Graphene-organic interactions can lead to strong doping [63,64,65,66], and to charge [67] or energy [68] transfer, making graphene a strong quencher of fluorescence of several organic molecules (Fig. 10b,c) such as pyrene [67,68] oligo- and poly-thiophene [33,69,70], poly-phenylenevinylene [70]. Even one SLG, GO or RGO can effectively quench the fluorescence of an organic thin layer [69], allowing to visualize single sheets with high optical contrast (~0.8) [69], or to quench fluorescent molecules at tens of nm away [71]. For more detailed reviews on graphene interactions with organic materials, see Refs. [72,73].

Graphene fabrication

The industrial exploitation of graphene will require large scale and cost-effective production methods, while providing a balance between ease of fabrication and final material quality. There are currently five main approaches: 1) mechanical exfoliation, 2) carbon segregation from carbon containing metal substrates and silicon carbide (SiC) 3) chemical vapour deposition (CVD) of hydrocarbons on reactive nickel or transition-metal-carbide surfaces, 4) chemical synthesis and 5) liquid phase exfoliation (LPE).

Exfoliation; Novoselov *et al.* introduced a manual cleaving process of graphite, frequently

called “mechanical exfoliation”, to obtain SLG and few layer graphene (FLG) [12,74]. This process makes use of adhesive tape to pull graphene films off a graphite crystal. When observed through an optical microscope, SLG and FLG add to the optical path compared to the bare substrate. If a proper SiO_2 thickness is chosen, the resultant visible contrast is sufficient to identify the number of layers [75,76,77,78]. Fig. 11b shows the result of a contrast simulation of SLG on SiO_2, where the contrast is plotted for a range of wavelengths and SiO_2 thicknesses [75]. In the visible range, SiO_2 films of ~90 nm and ~300 nm maximise contrast, hence are widely used as substrates. This pragmatic, low-cost method has enabled researchers to conduct a wide variety of fundamental physics and engineering experiments, even though it cannot be considered a process suitable for industrial exploitation (even though approaches for large scale mechanical exfoliation have been proposed). An example of typical exfoliated flake, with a varying number of layers, on an oxidized silicon wafer is shown in Fig. 11c. These layers have a slightly different colour in the optical microscope (Figure 11c). While a trained person can distinguish single- from few layer graphene by “naked eye” with high fidelity, Raman spectroscopy has become the method of choice when it comes to scientific proof of SLG [79,80]. Indeed, the graphene electronic structure is captured in its Raman spectrum that evolves with the number of layers [79]. The 2D peak changes in shape, width, and position for an increasing number of layers, reflecting the change in the electron bands via a double resonant Raman process. The 2D peak is a single band in SLG, whereas it splits in four bands in bi-layer graphene (BLG) [79]. This is demonstrated in Fig. 11d, where Raman spectra for SLG and FLG are plotted. Since the 2D peak shape reflects the electronic structure, twisted multi-layers can have 2D peaks resembling SLG, if the layers are decoupled.

The Raman spectrum of graphite was measured 42 years ago [81]. Since then Raman spectroscopy has become one of the most used characterization techniques in carbon science and technology, being the method of choice to probe disordered and amorphous carbons, fullerenes, nanotubes, diamonds, carbon chains, and polyconjugated molecules [82]. The Raman spectrum of graphene was measured 6 years ago [79]. This triggered a huge effort to understand phonons [79,80], electron-phonon [79,80,83], magneto-phonon [84,85] and electron-electron [86] interactions, and the influence on the Raman process of number [79] and orientation [79,80] of layers, electric [87,88,89] or magnetic [90,91] fields, strain [92, 93], doping [94,95], disorder[80], quality[96] and types [96] of edges, functional groups [97]. This provided key insights in the related properties of all sp^2 carbon allotropes, graphene being their fundamental building block. Raman spectroscopy has also huge potential for layered materials other than graphene.

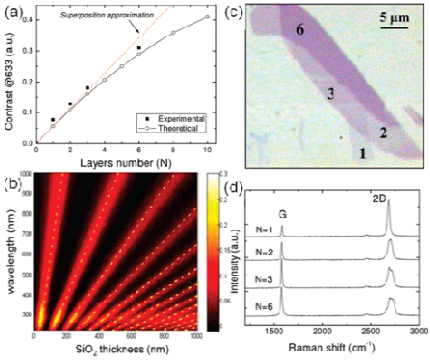

Fig. 11 > (a) Maximum contrast at 633 nm as a function of N. (b) Calculated contrast of graphene as a function of oxide thickness and excitation wavelength. Dotted lines trace the quarter-wavelength condition. c) Optical micrograph of multilayer with 1, 2, 3, and 6 layers. (d) Raman spectra as a function of number of layers.; From [75]./

Liquid phase exfoliation; Graphene flakes can be produced by exfoliation of graphite via chemical wet dispersion followed by ultrasonication, both in aqueous [98,99,100,101] and non-aqueous solvents [6,7,101,102]. This technique has the advantage of low cost and scalability. Graphene flakes with lateral sizes ranging from few nm to a few microns can now be produced with

concentration up to a few mg/ml in up to litre batches [102,103]. Control of lateral size and number of layers is achieved via separation in centrifugal fields. Up to ~70% SLG can be achieved by mild sonication in bile salts followed by sedimentation based-separation [100,104]. LPE also allows isolation of flakes with controlled thickness, when combined with density gradient ultracentrifugation (DGU) with~80% SLG yield (Fig.12) [99].

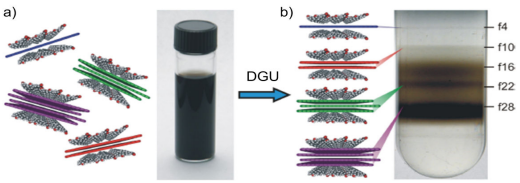

Fig. 12 > Sorting of graphite flakes using DGU. a) Schematic illustration of surfactant encapsulated graphene sheets and photograph of an unsorted aqueous. b) Photograph of a centrifuge tube following DGU marked with the main bands of monodisperse graphene [99]./

Other routes based on chemical wet dispersion have been investigated, such as exfoliation of fluorinated graphite [105], intercalated compounds [106], expandable graphite [107] ultrasonication of graphite in ionic liquid [103] and non-covalent functionalization of graphite with 1-pyrenecarboxylic acid [108].

LPE is an essential tool for the production of composite materials, thin films and conducting inks, with no need of expensive growth substrates. Graphene inks have been already demonstrated to be a viable route for the production of ink-jet printed thin film transistors [6]. Furthermore, many applications in photonics and optoelectronics, such as transparent conductors, third generation solar cell electrodes and optical graded graphene-based polymer composites will benefit from graphene produced by LPE [104]. LPE is also a useful for the production of graphene nanoribbons (GNR) [109]. LPE does not require transfer techniques and the resulting material can be deposited on different substrates (rigid and flexible) following different strategies such as, dip and drop casting, spin, spray and rod coating, ink-jet printing, etc.

LPE can also be used to exfoliate and disperse any other layered materials, such as chalcogenides and transition metal oxides (TMOs), BN, MoS_2, WS_2 etc. [110]. The development of a sorting strategy both in lateral dimensions and number of layers will be essential for the full exploitation of their optical and electronic properties.

Segregation form silicon carbide; Acheson reported a method for producing graphite from SiC in as early as 1896 [111]. Recently this approach has been perfected to yield SLG and FLG [112,113,114,115] (crystallites >10μm, small number of defects). Electronic decoupling from the underlying SiC substrate can be achieved by hydrogen treatment [116]. During the process, silicon is thermally desorbed at temperatures between 1250°C [112] and 1550°C [114,115]. This process is more controllable and scalable when compared to mechanical cleaving. In fact, graphene transistors can be manufactured from epitaxial graphene on a wafer scale [117]. Similar to exfoliated graphene, it has been demonstrated that single epitaxial graphene layers can be identified by Raman spectroscopy [118]. In addition Raman spectroscopy revealed that these layers are compressively strained [118]. A major disadvantage of epitaxial graphene is the high cost of SiC wafers, their limited size compared to Si wafers, and the high processing temperatures, well above current CMOS limits.

Chemical vapor deposition (CVD); SLG and FLG can be grown by CVD on metals, such as nickel [119,120,121,122], ruthenium [123] iridium [124,125] or copper [2,126]. Several methods of transferring the CVD graphene films onto target non-metallic substrates have been suggested [2,121,122], including the use of disposable Poly(methyl methacrylate) (PMMA) [121] or Polydimethylsiloxane (PDMS) [122] films.

CVD has now almost reached maturity for mass-production. Samples over 50 cm in size have been grown and transferred on target substrates [2].

Decisive progresses were made in the last few years towards the understanding of the growth processes, the characterization of the graphene/metal interaction, the tailoring of graphene's properties by tuning this interaction, or the design of novel hybrid structures with unique functionalities for spintronics, nanomagnetism, or catalysis. Europe occupies a special position in this respect, with a number of theory and surface science groups having pioneered the field.

Although CVD growth on Cu-foils is the most popular approach to date; there are other alternative schemes to produce wafer-scale graphene which yet require an active phase of research. Amongst these, are CVD on insulating substrates [127,128,129,130,131,132,133], Plasma Enhanced CVD (PECVD) [134] and molecular beam epitaxy (MBE) growth [135] .

Carbon segregation from metal substrates; This method exploits the solubility of carbon in transition metals (thin films of nickel), that subsequently segregates graphene at the metal surface. The graphene quality and the number of layers are strongly dependent on the growth and annealing conditions. The advantage of this method over standard CVD is that the graphene quality is controlled by the carbon source and annealing conditions. To get large metal grains with appropriate crystalline orientation (111) [136], a first step annealing of the metal surface is often performed. The carbon diffusion is simultaneously occurring during the crystalline orientation of nickel.

All the process steps occur in fully semiconductor compatible environment. Europe semiconductor industry can, then, reasonably take benefit of the versatility of this method toward the integration of graphene in their technological process flow.

Graphene growth by carbon segregation in Europe

This section exemplifies the leading and active position of Europe in graphene growth by carbon segregation. The first section deals with the study of the structural properties of graphene, the second addresses the investigation of the electronic, magnetic, and mechanical properties, the third focuses on the design of graphene/metal hybrid structures with novel functionalities, and the last gives an overview of Europe's efforts towards the production of graphene *via* growth on metals.

Structural properties of graphene/metals

Ref. 137 reported a pioneering atomic-scale characterization of SLG with scanning tunnelling microscopy (STM) in 1992, well before the “rise” of graphene. The study was performed for graphene grown on a Pt(111) crystal by chemical vapour deposition [137]. A number of European groups have employed this technique to study the structure of graphene on other metal surfaces, like Ir(111) (Fig. 13a) [138,139], Ru(0001) [140,141] or Ni(111) [142,143,144].

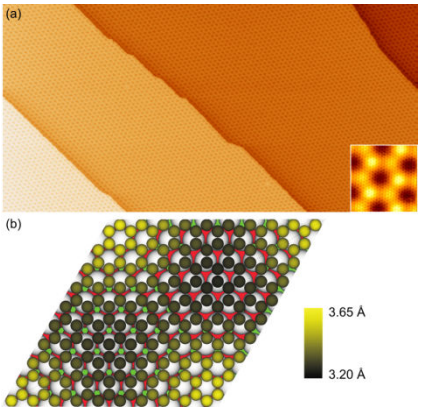

Fig. 13 > (a) 250×125 nm^2 STM topograph of graphene/Ir, showing the moiré superstructure spanning over four atomically flat terraces (from Ref. [124]); inset: atomic resolution STM topography showing the centre of carbon rings as dark spots, and the moiré superstructure, from [125]. (b) Top-view of the relaxed geometrical structure of graphene/Ir obtained by DFT including van der Waals interactions (from Ref. [145]).

Ref. [146] conducted surface X-ray diffraction (SXRD) measurements of SLG, and revealed a surprisingly large (ca 5 nm) commensurate graphene/Ru. Recent experiments also

revealed that incommensurate structures may be found as well, on graphene/Ir [145]. The question of commensurability of graphene onto metals is of fundamental nature. It has deep consequences, a wealth of intriguing phenomena related to the physics of phase transitions in two dimensions being expected. The graphene-metal distance and the nano-rippling of graphene on its metallic substrate, which follows the graphene-metal so-called moiré superstructure, are hallmarks of graphene-metal interaction: metals with a strong affinity with carbon are expected to induce a low graphene-metal distance [147], and a strong nano-rippling, which eventually can disrupt the conical band structure around the Fermi level and induce charge transfers.

This question fuelled an active debate in the literature. The contribution of Europe is decisive, and has much enriched the picture of the graphene/metal interaction thanks to the involvement of different groups with complementary expertises, ranging from STM [140,141], density functional theory (DFT) calculations [145,146,147,148,149], electron diffraction [150], He diffraction [151], SXRD [146], and more recently, X-ray standing waves [145].

There exist a long-lasting tradition of DFT simulations of carbon materials in Europe and this holds for graphene on metals. A pioneering contribution was in Ref. [136], who targeted the study of graphene on Ni(111). Large supercells (several hundred atoms) were considered in Ref. [145]. This is an unprecedented fine description of the graphene-metal electronic interaction [149]. Europe maintains its leading position, notably by its efforts towards taking into account van der Waals interactions in DFT [152,153], the most recent achievement being the use of a fully-consistent treatment of several hundred atoms supercells (Figure 13b) [145]. These interactions, often eluded in DFT calculations, are known to have prominent contribution to the graphene bonding on metals in many cases. Their implementation in DFT now provides a good description of the structure of graphene/metals, which agrees with the latest state-of-the-art measurements.

The production of high quality graphene via growth on metals first requires that defects in graphene are identified, then controlled, and whenever possible avoided. European groups have addressed, in some cases initiated, the study of a number of defects in graphene/metals: grain boundaries, pentagon-heptagon pairs [124], point defects [154], wrinkles [155], or local deformations [147].

Foreseen progress/evolution

The full understanding of the influence of defects on the properties of graphene has not been achieved yet. Benefiting from a strong expertise in defect characterization, Europe can play a crucial role in this respect. Answering the debated question of carbon magnetism due to vacancies in graphene would for instance be a major advance. Better controlling their formation and eventually avoiding them is of prime importance in view of producing ultra-high quality graphene. Another field where Europe could largely contribute to, based on its experience, is towards the graphene band structure engineering with the help of super-potentials induced by the graphene/metal epitaxy. Ordered vacancy lattices or antidot lattices, triangular or anisotropic moiré patterns, periodic strain patterns, etc, were proposed as efficient routes in this respect. Only a few of these routes were explored by experimentalists so far. Another area where Europe should continue is the understanding of the graphene/metal interaction, which drives the structure, electronic properties, and growth of graphene. A unified and predictive picture is still missing.

Electronic, magnetic, and mechanical properties of graphene/metals

It was realized a few years ago that the moiré pattern arising between graphene and metal substrate can act as a varying electronic potential for *n* [156]. This could induce nanometre-scale electron/hole pockets for

graphene/Ru [141]. The origin for these inhomogeneities is thought to be local charge transfers and change of hybridization [157]. Fainter modulations were found in graphene/Ir [158], where superpotential effects were evidenced by angle-resolved photoelectron spectroscopy (ARPES) (Fig. 14a) [158]. It was shown that the band structure can be further disturbed, up to the point where graphene π-bands become anisotropic, by metal cluster growth on graphene/Ir [156].

The study of the metal-graphene interactions started some years ago with ARPES [158]. Until 2009 however, only those metals which strongly interact with graphene were addressed. European groups conducted the first studies of graphene decoupled from its substrate [159].

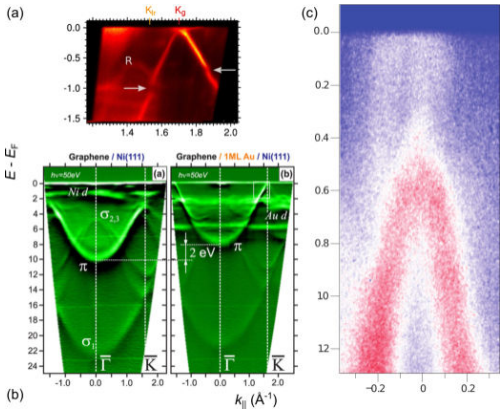

Fig. 14 > Energy (E) verus in-plane wave vectore ($k_{||}$) cuts in the band structure of graphene in the vicinity of the K point of graphene. The origin for the energy axis is taken at the Fermi level (E_F). (a) Graphene on Ir(111), showing a conical dispersion, marginal charge transfer, mini-band gaps (arrows) and a replica band, arising for moiré superpotential effects (from Ref. [158]), (b) graphene on Ni(111) (left) and with an intercalated Au layer (right), for which the conical dispersion of graphene is recovered (from Ref. [159]), (c) H-adsorbed graphene on Ir(111), characterized by the presence of a large band gap at the Dirac point (from Ref. [160])./

An almost intact Dirac cone, with a Dirac point almost matching the Fermi level (marginal charge transfer), was achieved for graphene on Ni intercalated by an Au monolayer (Fig. 14b) [159]. A similar observation was done for graphene on Ir (Fig. 14a) [158]. This pushed a number of groups worldwide to consider this system as a reasonable realization of free-standing graphene. Effective manipulating of graphene's band structure was put in evidence in this system, H adsorption inducing a bandgap, as high as 450 meV, at the Dirac point (Figure 14c) [160]; similar results were obtained for graphene/Au/Ni [161].

Spin-polarization of the π-bands could open the route to graphene-based spintronics. There has been a noticeable effort in this direction, restricted to Europe, which led to interesting debates. It was first argued that strong Rashba (spin-orbit) splitting of the π-bands could be induced in epitaxial graphene on Ni [144]. From other works, it is concluded that whether on Co or Ni, the Rashba splitting can only be marginal [162], while few 10 meV splitting was obtained via Au contact, which still corresponds to an enhancement of the spin-orbit constant in graphene by a factor of 100. The study of the thermal expansion coefficient of epitaxial graphene started recently [163]. Core level electron spectroscopy and *ab initio* molecular dynamics revealed an increase of the carbon bond length in a large range of temperature [164], and, counter-intuitively, an increase of the nano-rippling amplitude against heating [164]. SXRD confirmed that the graphene-metal epitaxy, even when governed by weak interactions, renders the thermal expansion coefficient different from that of isolated graphene, but does not follow that of the metal [147], possibly due to slippage.

The study of the nanomechanical properties of epitaxial graphene is again led by European groups. Atomic-scale resolution scanning probe microscopies, atomic force microscopy (AFM) [165] and STM [166] provided insights into local variations of the interaction between a metal tip and the graphene surface. The chemical inhomogeneity, which follows the Moiré and is due to varying interactions between graphene

and the substrate, were shown to play an important role. DFT calculations provided details of the electronic interaction between graphene and its metallic support. Many efforts in treating the spin degree of freedom in these calculations were pioneered by European groups [136,167,168,169]. This allowed addressing proximity induced magnetism, magnetic moment enhancement at the graphene/metal interface, or spinning filtering.

Foreseen progress/evolution

Beyond the exceptional thermal conduction of free-standing graphene, it is necessary to develop a good understanding of the thermal properties of graphene contacted to a metal, for instance in graphene/metal hybrid structures, or to elucidate the influence of metal electrodes contacted to graphene.

Epitaxial graphene on metals provides in certain cases model systems mimicking free-standing graphene. This is the case for graphene/Ir or Au intercalated graphene/Ni. The European community well understood this unique opportunity of taking benefit of the powerful tool-kit offered by surface science to probe the basic properties of graphene. Some of the properties remain mostly unexplored in epitaxial graphene, and it is reasonable to expect that Europe's state-of-the-art instrumentation should allow filling this gap.

Graphene/metal hybrid structures

The first proposals for graphene based spin-valves were reported in Europe [167]. Ref. [170] predicted that one or several graphene layers sandwiched between two epitaxial ferromagnetic leads (Figure 15a), was could offer high magnetoresistance and low resistance×area product [170] in the current-perpendicular-to-the-plane (CPP) geometry.

The latter feature is desirable for high density magnetic storage where small area ferromagnet/graphene/ferromagnet bits would have low resistance: low power consumption devices could thus be triggered. These theoretical works stimulated a strong interest in the community. Several groups are aiming at the experimental realization of the set-up. Along this view, a first step was made by a European group, with the demonstration of spin polarization in graphene on Ni [143].

The growth of flat and continuous layers of a ferromagnet on graphene is a difficult task since usually clustered films are formed. Using pulsed laser deposition it was found that high quality epitaxial ultrathin Co films could be prepared (Fig. 15b) [169]. Spin-valves in the CPP geometry now appear within reach.

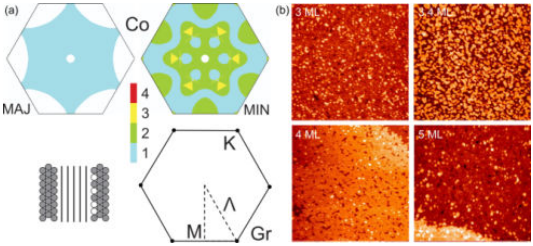

Fig. 15 > (a) Fermi surface (colour are for the number of Fermi surfaces) for Co minority and majority spin electrons (top), Fermi surface of graphene (bottom right), and schematic side-view of a graphene/Co spin valve (from Ref. [167]). (b) Layer-by-layer growth of Co by pulsed laser deposition on graphene/Ir, as seen by STM (100×100 nm^2 topographs), for increasing Co thickness, expressed in monolayers (ML) (from Ref. [169])./

Ref [138] has shown that epitaxial graphene may be decorated with dense arrays of equally sized nanoclusters, under the influence of the graphene/Ir moiré (Figure 13). Later the same group showed that a variety of materials could be organized on the moiré [163] (see Fig. 16), and other European groups reported that the method is also efficient on the graphene/Rh [171] and graphene/Ru [172] moirés. Not only these new systems pave way to the study of size dependent magnetic [39] or catalytic properties on a graphene substrate (*i.e.* potentially mediating exchange interactions or inert against catalytic reactions), but also the clusters may allow to manipulate the graphene band structure, as recently shown on graphene/Ir,

were anisotropic Dirac cones were accordingly engineered [156]. Worth noting also is the recent demonstration of supramolecular assemblies on epitaxial graphene [39,173], which could allow to engineer novel functionalities thanks to appropriate molecules.

Foreseen progress/evolution

Intercalation of a variety of elements between graphene and its metallic substrate has been studied for decades [174]. A few European groups started to make use of this effect in view of building-up novel graphene-based layered structures [159,168,169], either for protecting metal layers from atmosphere oxidation, or for tailoring graphene's band structure (band-gap, spin-splitting). Many progresses are expected in this direction, and novel complex heterostructures could be developed accordingly. The study of small-size effects (for instance catalytic or magnetic) and of the influence of the graphene substrate of cluster/graphene hybrids has just started.

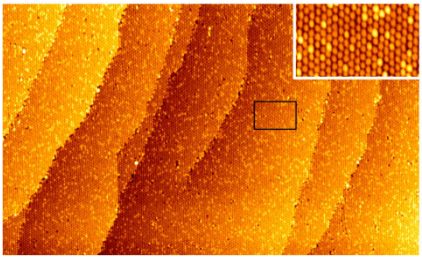

Fig. 16 >500*300 nm^2 STM topograph of Ir nanoclusters self-organized on the triangular moiré (2.5 nm pitch) of graphene/Ir(111). The inset shows a blow-up of the black-framed region (From Ref. [163])./

Europe occupies a leading position in this field. The interaction between physicists and chemists proved very efficient, as exemplified by the achievement and control of supramolecular networks on epitaxial graphene. Such fruitful interactions could extend to the surface chemical modification of graphene, which will provide new opportunities for tailoring the properties of graphene.

Graphene mass production

The investigation of the basic processes during graphene growth on metals is crucial in view of controlled growth of defect-free graphene over large areas. Europe, USA, Korea, Singapore, Japan and China are in strong and constructive competition in this field. Extensive STM work guided the achievement of centimetre-scale, single crystallographic orientation epitaxial graphene on Ir [124,175] or Ni [176], Pt [176], Ru [123,176]. Low-energy electron microscopy (LEEM), photoemission electron microscopy (PEEM) and spot profile low-energy electron diffraction (SPALEED) allowed to determine optimum growth conditions [155, 177, 178, 179]. Europe also offers unique STM instrumentation, with environmental microscopes operating at temperatures as high as 1000 K. This allowed real-time imaging of growth with nanometre resolution [180,181].

A recent evolution in the field of graphene production on metals consists in substrate engineering. The defects in the substrate are believed to influence the formation of defects in graphene. Low-cost preparation of large area graphene cannot afford bulk single-crystals as substrate. Almost simultaneously, a few research groups in US at University of Texas (R.S. Ruoff) [126], MIT (J. Kong) [121], in Korea at SAINT (B.H. Hong [122] and Sungkyunkwan University (J.H. Ahn) [2], together with two European teams [182,183] demonstrated the preparation of high quality graphene on thin, high quality metal films prepared on wafers.

Europe has a unique expertise in simulations of graphene (and CNT) growth on metal surfaces. The approach has been optimized along years and relies on tight binding Monte Carlo calculation. It allows tracking the initial stages of growth, and putting in evidence the formation precursors. Refs. [184,185] explored the temperature-dependent surface segregation of carbon contained in Ni [184,185], while Ref. [186] studied healing mechanisms for defects during growth [186].

European groups [182, 187, 188, 189, 190, 191, 192, 193, 194, 195] have contributed to the

optimization of chemical vapour deposition of graphene in low-cost conditions, *i.e.* at atmospheric pressures or slightly below. This preparation route efficiently provides large-area graphene of reasonable quality, after transfer to a suitable support. Given the few-months period required for preparation conditions optimization, it is expected that a number of additional reports/patents will be issued within Europe in the coming months. Controlled graphene nano-structuration is a long-standing quest which is motivated by the prospect for band gap creation in graphene. This is a prerequisite for logic graphene transistors. Ref. [196] suggested surface polymerization at metal surfaces. The next step consists in transferring GNRs to appropriate supports. Even if CVD on metal is a very promising mass production technique, the transfer step could be considered as an issue. Polymer transfer (by PMMA and PDMS) may leave some impurities.

Moreover, the Cu foil which is mostly used to produce large SLG is expensive and can impact the whole process specification. An efficient Cu recycling strategy needs to be devised.

Europe can play a major role in looking for rapid, cheap and versatile fabrication methods. Europe leads LPE of graphene [7]. This technique was developed there, and several advances have been achieved [98,100,102,103,104,106]. LPE needs to be improved to reach control on-demand of number of layers, flakes thickness and lateral size, as well as the rheological properties of the graphene dispersions. Modelling is needed to fully understand the exfoliation process in different solvents, in order to better separate flakes in centrifugal fields, so to achieve SLG and FLG with well defined morphological properties at a high rate.

Foreseen progress /evolution

Europe is strongly involved in *in situ* studies of the growth of epitaxial graphene. It is possible that that this will allow Europe to be a key player in the highly competitive field of graphene growth of metals. Noteworthy, growth monitoring *in operando*, *i.e.* close to 1000°C, either under UHV or atmospheric conditions, is being pursued by several EU labs.

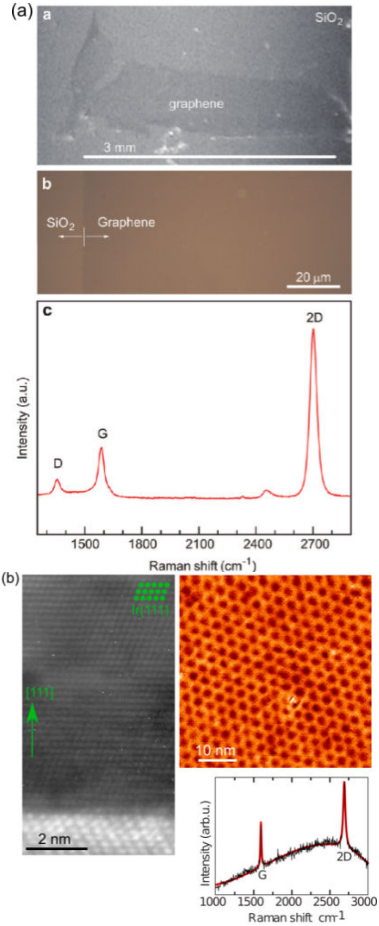

Fig. 17 > (a) Graphene transferred from its high quality Ni thin film on MgO: optical micrographs (top and middle) and Raman spectrum of graphene transferred on a Si/SiO_2 wafer (from Ref. [181]). (b) Transmission electron microscope cross-section of a single crystalline Ir(111) thin film on C-plane sapphire (left), STM topograph of a graphene layer on top of this film (top right), and Raman spectrum of graphene/Ir (bottom right) (from Ref. [168]).

Europe position in graphene chemistry

Europe is strong in graphene chemistry research, with several groups leading the fields

of covalent and supramolecular functionalization. The recent production of mono-dispersed, tuneable graphene nano-ribbons with controlled edge terminations by bottom-up chemical synthesis [28] is a major, all-European advancement in the field. Another recent European advance is the selective chemical functionalization of the graphene edges [34]. Graphene chemistry is also strongly pursued by major European companies, collaborating in different FP7 projects.

Bottom-up graphene design

Precise control of the GNR edge structure is essential to avoid defect induced scattering [28]. One promising route is bottom-up growth via polymerisation of polyaromatic oligomers (Figure 18). Ref. [197] successfully produced a variety of GNRs using metal assisted coupling of molecular precursors into linear polyphenylenes, followed by cyclodehydrogenation.

While there are currently scalability issues with this approach, nevertheless it shows great promise, especially in view of controllable edge site chemical functionalization, for chemical fine tuning of nanoribbon electronic properties.

Alternative routes to control edge chemistry are under development, for example top-down approaches exploiting metal nanoparticles to selectively etch graphene with crystallographic orientation [198,165] or via STM lithography [199,166]. Ribbon edge and defect chemistry is being driven in Europe by first principles electronic structure modelling [200,167]. Edge chemistry and structure dominates the band gap of GNRs [201,168], with out-of-plane distortions stabilizing the edges [202,203,169,170]. Selective edge functionalisation was proposed as a route to nanojunction design in GNRs [204,171], while quantum transport modelling suggests that controlled GNR doping with light element impurities, such as Ni and B may be a route to new types of switching devices [167,205,172]. Further work on defect modelling is summarised in a recent review [205].

The combination in Europe of a well established community of atomic scale modelling, with strong expertise in controlled nanocarbon chemistry offers an exciting potential for bottom-up design of graphene based materials and devices.

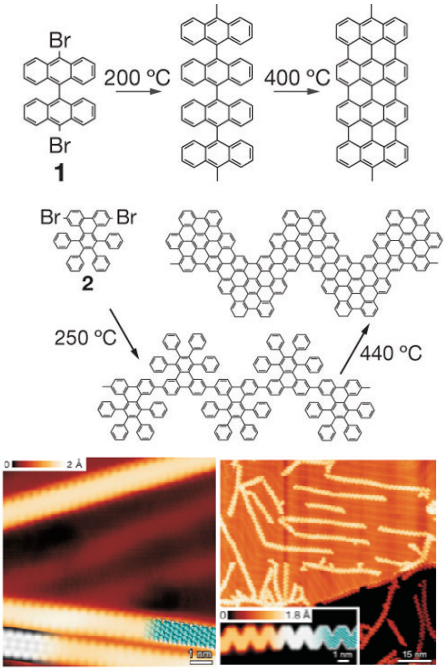

Fig. 18 > (top) Reaction schemes for producing straight and chevron-type graphene nanoribbons on metal surfaces using different molecular precursors, (bottom left) High resolution STM with overlaid molecular model (blue) of resultant graphene nanoribbon (T=5K, U=-0.1V, I=0.2nA), (bottom right) Overview STM image of chevron-type graphene nanoribbons fabricated on a Au(111) surface (T=35K, U=–2V, I=0.02nA). The inset shows a high-resolution STM image (T=77K, U=–2V, I=0.5nA) and a DFT-based simulation of the STM image (greyscale) with partly overlaid molecular model of the ribbon (blue, carbon; white, hydrogen). From [28]./

Nomenclature and classification

As the graphene field matures and becomes increasingly applications driven, new standards and classifications will be needed, for which the integrated research community within Europe is well placed to act as a driving force.

Low cost ‘industrial graphene’ for composite applications may contain multi-layer material,

whilst ICT-grade graphene requirements will be more stringent. Flake size, impurity content, degree of poly-crystallinity and chemical post-treatment will all need to be incorporated in such a classification. As for any other carbon material [206], Raman spectroscopy [207,208,209] may be the ideal tool to provide a standard reference.

Graphene photonics and optoelectronics

Graphene is emerging as a viable alternative to conventional optoelectronic, plasmonic and nanophotonic materials [104]. It has decisive advantages such as near-wavelength-independent absorption, tunability via electrostatic doping, large charge-carrier concentration, low dissipation rates, extraordinary electronic properties and the ability to confine electromagnetic energy to unprecedented small volumes. Graphene can be produced in large quantities and large areas, a key ingredient towards future graphene-based photonics. In addition, it can also be integrated with Si technology on a wafer-scale. Combined, these aspects constitute fundamental advantages to produce photonic devices with performance superior to other materials, especially in less-conventional wavelength ranges, thus far limited by the unavailability of appropriate optical materials.

Transparent conductors/contacts

Graphene and other 2d layered materials, will have a disruptive impact on current optoelectronics devices based on conventional materials, not only because of cost/performance advantages, but also because they can be manufactured in more flexible ways, suitable for a growing range of applications. In particular, human interface technology requires the development of new applications based on stretchable electronics and optoelectronics, such as flexible displays, touch-screens, light emitting diodes, conformal biosensors, photodetectors and new generation solar cells. Such devices are mostly based on transparent conducting electrodes (TCEs) that require materials with low Rs and high T throughout the visible region, other than physical and chemical stability, appropriate work function, uniformity, thickness, durability, toxicity and cost [210].

The dominant material used in TC applications is ITO [211]. This has limitations: an ever increasing cost due to In scarcity [211], processing requirements, difficulties in patterning [211,212], sensitivity to acidic and basic environments. Moreover, ITO is brittle and can wear out or crack when bending is involved, such as touch screens and flexible displays [213]. Metal grids [214], metallic nanowires [215], or other metal oxides [212] have been explored as alternative. Metal nanowires, e.g. Ag NWs have been demonstrated as TCEs on polymeric substrates using different methods, such as vacuum filtration, rod coating, transfer printing, and spray deposition. However, they suffer from stability and adhesion issues. On the other hand, 2d layered materials are ideal candidates offering a cost-effective, flexible alternative to ITO and other transparent conductors. Graphene in principle can combine high T with high conductivity, maintaining these properties even under extreme bending and stretching, ideal for easy integration in polymeric and flexible substrates. In many cases (e.g. touch screens or OLEDs), this increases fabrication flexibility, in addition to having economic advantages. For instance, present liquid-crystal-based devices face high fabrication costs associated with the requirement for large transparent electrodes. The move to a graphene-based technology could make them more viable. New forms of graphene-based TCEs on flexible substrates for solar cells add value and operational flexibility, not possible with current TCs and rigid glass substrates.

Doped graphene offers comparable T and Rs to ITO on flexible substrates [212]. Graphene films have higher T over a wider wavelength range with respect to CNT films [216,217,218], thin metallic films [214,215], and ITO [212], Fig. 19a. However, the bi-dimensional dc conductivity $\sigma_{2d,dc}$ does not go to zero, but assumes a

constant value [12] $\sigma_{2d,dc}$~$4e^2/h$, resulting in Rs ~6kΩ for an ideal intrinsic SLG with T ~97.7%. Thus, ideal intrinsic SLG would beat the best ITO only in terms of T, not Rs. However, real samples deposited on substrates, or in thin films, or embedded in polymers are never intrinsic. Exfoliated SLG has typically $n \geq 10^{12} cm^{-2}$ (see e.g. Ref [219]), and much smaller Rs. Figs. 19b,c show that graphene can achieve the same Rs as ITO, ZnO-Ag-ZnO [220], TiO_2/Ag/TiO_2 and CNTs with a much reduced thickness (Fig 19b) and a similar, or higher T. Fig. 19c plots T versus Rs for ITO [214], Ag nanowires [214], CNTs [216] and the best graphene-based TCFs reported to date [2], again showing that the latter is superior. For instance, taking $n=3.4\times10^{12} cm^{-2}$ and $\mu=2\times10^4 cm^2/Vs$, achievable in CVD sample, it is possible to get T=90% and Rs = 20Ω/□ [104] with graphene, values already achieved with hybrid graphene-metal grids [221].

Different strategies were explored to prepare graphene-based TCFs: spraying [46], dip [222] and spin coating [44], vacuum filtration [223], roll-to-roll processing [2]. Huge progresses were made since the first TCs using GO [223]. A key strategy to improve performance is stable chemical doping. For instance, Ref. [2] achieved Rs ~30Ω/□; T~90% by nitric acid treatment of GTCFs derived from CVD grown flakes, which is one order of magnitude lower in terms of Rs than previous GTCFs from wet transfer of CVD films. Acid treatment permitted to decrease the Rs of solution processed nanotubes-graphene hybrid film till 100Ω/□ for T=80% [224]

Figure 19d is an overview of current graphene-based TCs. It shows that GTCFs derived from CVD, combined with doping, could outperform ITO, metal wires and SWNTs.

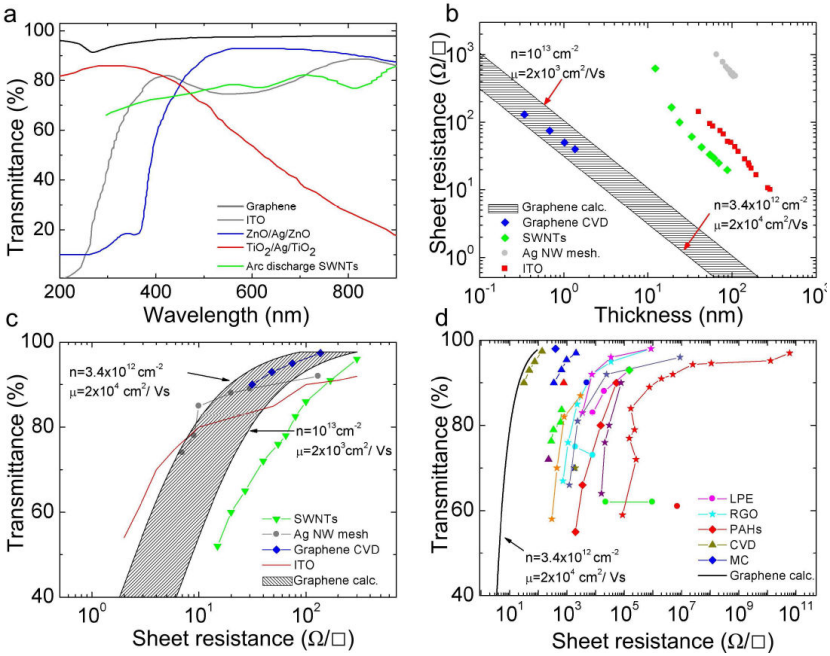

Fig. 19 > a) Transmittance of graphene compared to different transparent conductors; b) Thickness dependence of Rs for graphene compared to some common materials; c) T vs Rs for different transparent conductors compared to graphene; d) T vs Rs for GTCFs grouped according to production strategies: CVD, micro-mechanical cleavage (MC), organic synthesis using poly-aromatic hydrocarbon (PAHs), LPE of pristine graphene or graphene oxide (GO). A theoretical line is also plotted for comparison [226]./

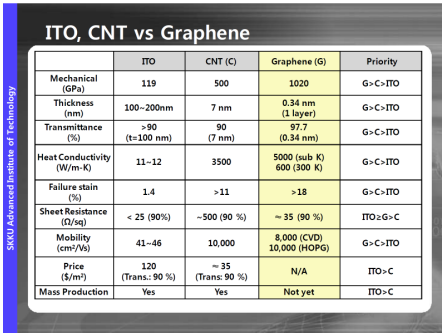

	ITO	CNT (C)	Graphene (G)	Priority
Mechanical (GPa)	119	500	1020	G>C>ITO
Thickness (nm)	100~200nm	7 nm	0.34 nm (1 layer)	G>C>ITO
Transmittance (%)	>90 (t=100 nm)	90 (7 nm)	97.7 (0.34 nm)	G>C>ITO
Heat Conductivity (W/m-K)	11~12	3500	5000 (sub K) 600 (300 K)	G>C>ITO
Failure stain (%)	1.4	>11	>18	G>C>ITO
Sheet Resistance (Ω/sq)	< 25 (90%)	~500 (90 %)	~ 35 (90 %)	ITO≥G>C
Mobility (cm^2/Vs)	41~46	10,000	8,000 (CVD) 10,000 (HOPG)	G>C>ITO
Price ($/$m^2$)	120 (Trans.: 90 %)	~ 35 (Trans: 90 %)	N/A	ITO>C
Mass Production	Yes	Yes	Not yet	ITO>C

Fig. 20 > Comparison between performances of ITO, carbon nanotubes and graphene (by courtesy of Byung Hee Hong Seoul National./

Note that GTCFs and GOTCFs produced by other methods, such as LPE, albeit presently with higher Rs at T=90%, have already been tested in organic light emitters [225], solar cells [222] and flexible smart window [104]. These are a cheaper and easier scalable alternative to CVD films, and need be considered in applications where cost reduction is crucial. Figure 20 summarizes the main properties of graphene TCEs comparing the performances with respect to ITO and CNTs [226].

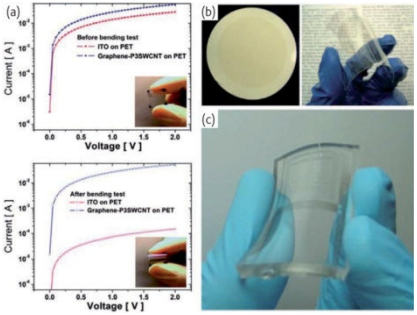

Fig. 21 > Preserving electrical conductivity under stress is an important property for TCFs. (a) Upon flexing the conductivity of indium tin oxide decreases 3 orders of magnitude, while the conductivity of a G-CNT hybrid electrode remains stable. From [227]./

The aforementioned performances of graphene-based TCEs are extremely promising in view of commercial applications, especially in bendable and stretchable devices (see fig.21), e.g. as window electrode in inorganic (fig. 22a), organic (fig. 22b) and dye-sensitized solar cells (fig. 22c) other than in OLED (fig. 22d) touch screen (fig. 22e) smart window (fig. 22f), etc.

Photovoltaic devices

The direct exploitation of solar radiation to generate electricity in photovoltaic (PV) devices is at the centre of an ongoing research effort to utilize the renewable energy. Si currently dominates the market of PV devices [228], with energy conversion efficiency (η) up to ~25% [229]. However, regardless of significant development over the past decades [230], the high cost of Si-based solar cells is a bottleneck for the implementation of solar electricity on large scale (in absence of government subsidies). The development of new PV materials and concepts is thus fundamental to reduce the overall costs and increase efficiency.

Graphene can fulfil multiple functions in photovoltaic devices: TC window, antireflective layer, photoactive material, cannel for charge transport and catalyst [104]. GTCFs can be used as window electrodes in inorganic [231], organic [232] and dye-sensitized solar cells (DSSCs) [222], see fig. 22 a,b,c respectively. The best performance achieved to date has η≈ 1.2% using CVD graphene as the TC, with Rs values of 230Ω/□ and T=72% [233]. However, further optimization is certainly possible, considering that GTCFs with Rs=30Ω/□ and T=90% have already been demonstrated [2] and graphene-hybrids have been reported with even better results (Rs 20Ω/□, T=90%) [221].

GO dispersions were also used in bulk heterojunction photovoltaic devices, as electron-acceptors achieving η≈1.4% [234]. Theoretically η~12% should be possible with graphene as photoactive material [235].

Graphene can cover an even larger number of functions in DSSCs. Indeed, other than as TC window [222], graphene can be incorporated into the nanostructured TiO_2 photoanode to enhance the charge transport rate, preventing recombination, thus improving the internal photocurrent efficiency [236]. An efficiency of

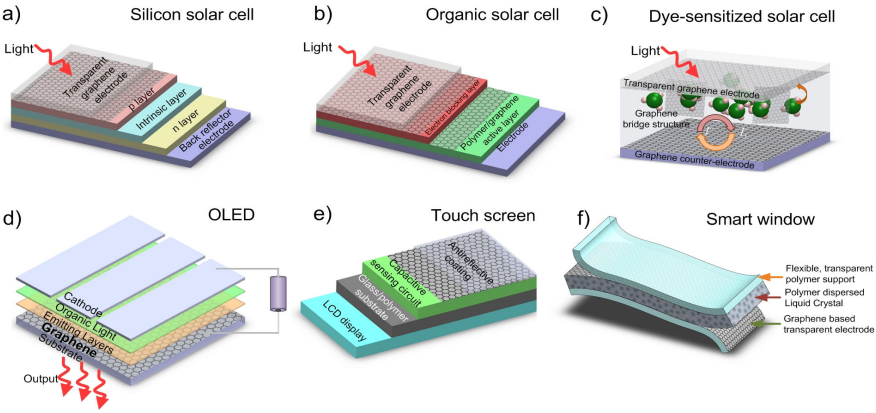

Fig. 22 > Graphene-based optoelectronics. Schematics of inorganic (a), organic (b) and dye-sensitized (c) solar cells, organic LED (d) capacitive touch screen (e) and smart window (f) [104]./

~7%, higher than conventional nanocrystalline TiO_2 photoanodes in the same experimental conditions, was demonstrated in Ref. [236]. Graphene quantum dots with tuneable absorption have been designed, produced and demonstrated as promising photoactive materials in DSSCs [237]. Further optimization is required for the optimum adsorption of these molecules with TiO_2 nanoparticles by covalently attaching binding groups to the quantum dots in order to improve charge injection. Another option is to use graphene, with its high surface area [238], as substitute for the platinum (Pt) counter-electrode. A hybrid poly(3,4 ethylenedioxythiophene):poly(styrenesulphonate) (PEDOT:PSS) graphene oxide composite was used as counter-electrode, to obtain η = 4.5%, comparable to the 6.3% for a Pt counter-electrode tested under the same conditions [239] but now with a cheaper material. More importantly, it was recently demonstrated that graphene can be used as counter-electrode material to replace simultaneously both Pt as catalyst and the TC oxide as conductive electrode [240]. This is a fundamental step towards cost reduction and large scale integration of DSSCs.

Current solar cell technologies use only a small part of the solar spectrum [212], due to their intrinsic band gap limiting the maximum detectable wavelength. The absence of a band-gap in graphene translates into the absence of this detectable wavelength limit. This means that solar radiation over a much wider spectral range could be converted to energy.

The combination of graphene with plasmonic nanostructures can also be used to increase the light harvesting properties in solar cells [241].

Organic Light Emitting Diodes

Organic light-emitting diodes (OLEDs) are a class of optoelectronic devices that can take advantage of graphene. Low power consumption and ultra-thin OLEDs have been developed more than 20 years ago [242], and are now applied in ultra-thin televisions and other displays, such as those on digital cameras and mobile phones.

OLED have an electroluminescent layer between two charge- injecting electrodes, at least one of which transparent. In these diodes, holes are injected into the highest occupied molecular orbital (HOMO) of the polymer from the anode, and electrons into the lowest unoccupied molecular orbital (LUMO) from the cathode. For efficient injection, the anode and cathode work functions should match the HOMO and LUMO of the light-emitting

polymer. Traditionally, ITO is used as the transparent conductive film. However, it has a number of disadvantages. First, ITO may be too expensive for use in OLEDs for lighting because of the increasing cost and the low throughput deposition process. Second, metal oxides such as ITO are brittle and therefore of limited use on flexible substrates. Third, In is known to diffuse into the active layers of OLEDs, which leads to a degradation of performance over time. There is a clear need for alternative TCEs with optical and electrical performance similar to ITO but without its drawbacks. Graphene has a work function of 4.5 eV, similar to ITO. This, combined with its promise as a flexible and cheap transparent conductor, makes it an ideal candidate for an OLED anode (fig. 22d), while also eliminating issues related to In diffusion.

Ref [243] developed an OLED with a few nanometers of graphene as transparent conductor. Ref [244] reported a flexible OLED based on a modified graphene anode having a high work function and low Rs. The performance (37.2 lm W^{-1} in fluorescent OLEDs, 102.7 lm W^{-1} in phosphorescent OLEDs) outperforms optimized devices with an ITO anode (24.1 lm W^{-1} in fluorescent OLEDs, 85.6 lm W^{-1} in phosphorescent OLEDs) [244].

These results pave the way for inexpensive OLED mass production on large-area low-cost flexible plastic substrates, which could be rolled up like wallpaper and applied to any substrate

Touch screens

Touch panels are used in a wide range of applications, such as cell phones and cameras, and where keyboard and mouse do not allow a satisfactory, intuitive, quick, or accurate interaction with the display content.

Resistive and capacitive (see fig. 22e) touch panels are the most common. A resistive touch panel comprises a conductive substrate, a LCD front-panel, and a TCF [245]. When pressed by a finger or pen, the front-panel film comes into contact with the bottom TC and the coordinates of the contact point are calculated on the basis of their resistance values. The TC requirements for resistive screens are Rs ~500−2000Ω/□ and T>90% at 550nm [245]. Favourable mechanical properties, including brittleness and wear resistance, high chemical durability, no toxicity, and low production costs are also important. GTCFs can satisfy the requirements for resistive touch screens in terms of T and Rs, when combined with large area uniformity. Ref. [2] reported a graphene-based touch panel by screen-printing a CVD sample. Considering the Rs and T required by analogue resistive screens, GTCF or GOTCF produced via LPE also offer a viable alternative, and further cost reduction.

Capacitive touch screens are emerging as the high-end version, especially since the launch of Apple's iPhone. These consist of an insulator such as glass, coated with ITO [245]. As the human body is also a conductor, touching the surface of the screen results in electrostatic field distortion, measurable as a change in capacitance. Although capacitive touch screens do not work by poking with a pen, thus mechanical stresses are lower with respect to resistive ones; the use of GTCFs can improve performance and reduce costs.

However, these solutions do not yet provide 100% satisfaction in terms of user experience, as touch screens tend to be inert in the way they interact with a user. Also, the proliferation of icons, virtual keys and densely packed browsing menus on mobile touch screen displays require increasing cognitive efforts from the user in order to be located, distinguished and manipulated. Solutions for low-cognitive effort user interfaces (UI), such as vibration enabled tactile feedback, are currently gaining market momentum by improving usability, interaction interoperability, and user acceptance.

Thus far, most active tactile feedback solutions have been implemented through simple monolithic vibrations of the entire device driven by a single or very few vibrating actuators, typically electromechanical or piezoelectric [246]. The types of tactile

feedback that can be provided by such traditional techniques are limited to relatively basic feedback patterns which are only partially correlated to finger position, perceived audio-visual information and actions. Such solutions do not yet provide complete satisfaction in terms of user experience. Key to this is the inability of monolithic vibrations to provide localized tactile feedback associated with visual images, and this is related to the difficulty in implementing tactile feedback directly from a display surface. To address the problem of providing localized tactile feedback directly from the display of a device, a flexible and optically transparent graphene-based programmable electrostatic tactile (ET) system was developed [247] capable of delivering localized tactile information to the user's skin, directly from the display's surface and in accordance with the displayed visual information. The device is based on the electrovibration a phenomenon [248] that can be explained through electrostatic interaction between the touch surface and the user finger [249].

Graphene photodetectors

Photodetectors measure photon flux or optical power by converting the absorbed photon energy into electrical current. They are widely used in a range of devices [250], such as integrated optoelectronic circuits, televisions, DVD players, biomedical imaging, remote sensing and control, optical communications, and quantum information technology. Most exploit the internal photoeffect, in which the absorption of photons results in carriers excited from the valence to the conduction band, outputting an electric current. The spectral bandwidth is typically limited by the absorption [250]. Graphene absorbs from the UV to THz [24,251,252,253]. As a result, graphene-based photodetectors (GPD) (fig. 23) could work over a much broader wavelength range. The response time is ruled by the carrier mobility. Graphene has huge mobilities, so it can be ultrafast [251]. Graphene's suitability for high-speed photodetection was demonstrated in an comms link operating at 10Gbit s^{-1}[254].

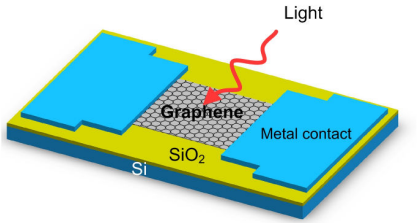

Fig. 23 > Graphene-based photodetector [104]./

The photoelectrical response of graphene has been investigated both experimentally and theoretically [254,255,256,257,258]. Although the exact mechanism for light to current conversion is still debated [256,259,260], a p–n junction is usually required to separate the photo-generated e–h pairs. Such p–n junctions are often created close to the contacts, because of the difference in the work functions of metal and graphene [148,261]. Responses at wavelengths of 0.514, 0.633, 1.5 and 2.4μm have been reported [255]. Much broader spectral detection is expected because of the graphene ultrawideband absorption [258]. The operating bandwidth of GPDs is mainly limited by their time constant resulting from the device resistance, R, and capacitance, C. An RC-limited bandwidth of about 640 GHz was reported for graphene [258], comparable to traditional photodetectors [262]. However, the maximum possible operating bandwidth is typically restricted by their transit time, the finite duration of the photogenerated current [250]. The transit-time-limited bandwidth of graphene photodetectors could be over 1,500 GHz [258].

Although an external electric field can produce efficient photocurrent generation with an electron–hole separation efficiency >30% [256], zero source–drain bias and dark current operations could be achieved by using the internal electric field formed near the metal electrode–graphene interfaces [254,223]. However, the small effective area of the internal electric field could decrease the detection efficiency [214,262], as most of the generated electron–hole pairs would be out of the electric field, thus recombining, rather than being separated. The internal photocurrent

efficiencies (15−30% [256,257] and external responsivities (generated electric current for a given input optical power) of ~6.1 mA/W, much higher than the so far reported [254] for GPDs are relatively low compared with current photodetectors [250]. This is mainly due to limited optical absorption when only one SLG is used, short photocarrier lifetimes and small effective areas (~200 nm [258]).

Future work will target the low light absorption of graphene (2.3% of normal incident light [24,263]), the difficulty of extracting photoelectrons (only a small area of the p–n junction contributes to current generation); and the absence of a photocurrent for the condition of uniform flood illumination on both contacts of the device. Unless the contacts are made of different materials, the voltage/current produced at both contacts will be of opposite polarity for symmetry reasons, resulting in zero net signal [254,256,264].

The optimization of the contacts needs to be pursed both theoretically and experimentally. Other possible ways of overcoming these restrictions is to utilize plasmonic nanostructures placed near the contacts as recently demonstrated [241]. Such a field enhancement, exactly in the area of the p–n junction formed in graphene, can result in a significant performance improvement.

The significant photothermoelectric contribution to the photocurrent in graphene p-n junctions was recently pointed out [260]. This regime, which features a long-lived and spatially distributed hot carrier population, may offer a path to hot carrier–assisted thermoelectric technologies for efficient solar energy harvesting.

Recently, a novel hybrid graphene-quantum dot phototransistor with ultrahigh gain has been demonstrated [265]. The proposed device takes advantage of the strong light absorption in quantum dots and the two-dimensionality and high mobility [20] of graphene to merge these materials into a hybrid system for photodetection with extremely high sensitivity [265]. The graphene-quantum dot phototransistor has shown ultrahigh gain of 10^8 and ten orders of magnitude larger responsivity with respect to pristine graphene photodetectors [265]. Moreover, the hybrid graphene-quantum dot phototransistors exhibit spectral selectivity from infrared to visible, gate-tunable sensitivity, and can be integrated with current circuit technologies [265].

Graphene was also demonstrated to be ideal for the enclosure within a planar λ/2 optical microcavity [266]. The latter is a photonic structure that confines optical fields between two highly reflecting mirrors with a spacing of only one half wavelength of light [267]. The optical confinement provide a powerful means to control both the otherwise featureless optical absorption [24] and the spectrally broad thermal emission [268,269] of graphene. The monolithic integration of a graphene transistor with a planar optical microcavity permitted the control on photocurrent generation. Tuning the excitation wavelength on resonance with the optical microcavity, an enhancement of ~20 in photocurrent was measured with respect to the out of resonance excitation [266]. In the same condition (spectral interval) a non-confined graphene transistor has shown a photocurrent increase of only 2. This demonstrates that the mocrocavity-controlled graphene transistor acts as light detector with spectral selectivity [266].

Moreover, electrically excited, thermal light emission of graphene can be controlled by the spectral properties of the microcavity. Indeed, the thermal emission spectrum of a microcavity-controlled graphene transistor displays a single, narrow peak at λ_{cavity}= 925nm having a fullwidth-at-half-maximum of 50 nm, providing a 140-fold spectral narrowing with respect to the simulated free-space thermal spectrum at T = 650 K [266].

Moreover, the integrated graphene transistor electrical transport characteristic is profoundly modifies by the optical confinement of graphene by the optical microcavity [266]. The modifications of the electrical transport can be

related to the microcavity-induced enhancement or inhibition of spontaneous emission of thermal photons [266]. The concept of optical confinement of graphene enables a new class of functional devices as, for example, spectrally selective and highly directional light emitters, detectors, and modulators.

Graphene saturable aborbers

Materials with nonlinear optical and electro-optical properties are needed in most photonic applications. Laser sources producing nano- to sub-picosecond pulses are key components in the portfolio of leading laser manufacturers. Regardless of wavelength, the majority of ultrafast lasers use a mode-locking technique, where a nonlinear optical element, called a saturable absorber, turns the continuous-wave output into a train of ultrafast optical pulses [270]. The key requirements are fast response time, strong nonlinearity, broad wavelength range, low optical losses, high power handling, low power consumption, low cost and ease of integration into an optical system. Currently, the dominant technology is based on semiconductor saturable absorber mirrors (SESAM) [270,271]. However, these have a narrow tuning range, and require complex fabrication and packaging [270,272]. The linear dispersion of the Dirac electrons in graphene offers an ideal solution: for any excitation there is always an electron–hole pair in resonance. The ultrafast carrier dynamics [273,274] combined with large absorption [24,75] and Pauli blocking, make graphene an ideal ultrabroadband, fast saturable absorber [253,272]. Unlike SESAM and CNTs, there is no need for bandgap engineering or chirality/diameter control [253,272].

Since its first demonstration in 2009 [272], the performance of ultrafast lasers mode-locked by graphene has improved significantly (Fig.24). For example, the average output power has increased from a few mW [272] to 1 W [275]. Some of the aforementioned production strategies (e.g. LPE [101,253,272,276,277,278], CVD [279,280], carbon segregation[281], mechanical exfoliation [282,283]) have been used for graphene saturable absorber (GSA) fabrication. So far, GSAs have been demonstrated for pulse generation at 1μm [275,284], 1.2μm [285], 1.5μm [253, 272, 279, 280, 282, 286] and 2μm [287]. The most common wavelength so far is ~1.5μm, not due to GSAs wavelength restriction, but because this is the standard wavelength of optical telecommunications. Ref. [288] reported a widely tunable fiber laser mode-locked with a GSA demonstrating its "full-band" operation performance. For fiber lasers, the simplest and most economical approach to GSA integration is sandwiching it between two fiber connectors (Fig.24) [253, 272, 279, 280, 282, 283, 288]. Other GSA integration approaches (e.g. evanescent-wave based integration [287]) have been demonstrated for high-power generation. Sub-200fs pulses have been achieved using a stretched-pulse design, where the cavity dispersion is balanced to stretch the pulse for the limitation of nonlinear effects [276].

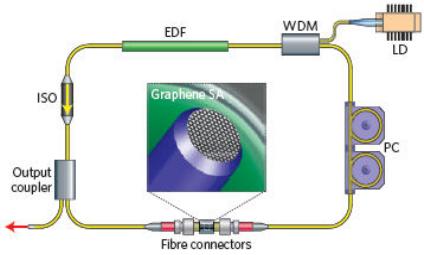

Fig. 24>Graphene mode-locked fiber. WDM, wavelength division multiplexer; PC, polarization controller; EDF, erbium-doped fiber; ISO, isolator [77]./

Solid-state lasers are typically used for high-power output, as alternative to fiber lasers [289]. GSAs have also been demonstrated to mode-lock solid-state lasers [284,285,290]. In this case, CVD graphene (>1cm^2) has been directly transferred to quartz for solid-state laser mode-locking [285]. Ref. [285] reported 94fs pulses with 230mW output power. Another approach for GSA fabrication relies in spin-coating LPE graphene either on quartz substrates or high-reflectivity mirrors. GSA can

then be inserted into a solid-state cavity for ultrafast pulse generation achieving average power up to 1W using a solid-state Nd: YVO4 laser [275]. The output wavelength is ~1 μm with power energy of ~14nJ.

Optical limiters and frequency converters

Optical limiters are devices that have high transmittance for low incident intensity and low transmittance for high intensity [291]. There is a great interest in these for optical sensors and human eye protection, as retinal damage can occur when intensities exceed a certain threshold [291]. Passive optical limiters, which use a nonlinear optical material, have the potential to be simple, compact and cheap [291]. However, so far no passive optical limiters have been able to protect eyes and other common sensors over the entire visible and near-infrared range [291]. Typical materials include semiconductors (i.e. ZnSe, InSb), organic molecules (i.e. phthalocyanines), liquid crystals and carbon-based materials (i.e. carbon-black dispersions, CNTs and fullerenes) [291,292]. In graphene-based optical limiters the absorbed light energy converts into heat, creating bubbles and microplasmas [292], which results in reduced transmission. Graphene dispersions can be used as wideband optical limiters covering visible and near-infrared. Broad optical limiting (at 532 and 1,064 nm) by LPE graphene was reported for nanosecond pulses [292]. It was also shown [293] that functionalized graphene dispersions could outperform C60 as an optical limiter.

Optical frequency converters are used to expand the wavelength accessibility of lasers (for example, frequency doubling, parametric amplification and oscillation, and four-wave mixing) [291]. Calculations suggest that nonlinear frequency generation in graphene (harmonics of input light, for example) should be possible for sufficiently high external electric fields (>100 V cm^{-1}) [294].

Second-harmonic generation from a 150fs laser at 800nm has been reported for a graphene film [295]. In addition, four-wave mixing to generate near-infrared wavelength tunable light has been demonstrated using SLG and FLG [296]. Graphene's third-order susceptibility $|\chi 3|$ was measured to be ~10^{-7} e.s.u. [296]—up to one order of magnitude larger than CNTs [296]. Other features of graphene, such as the possibility of tuning the nonlinearity by changing the number of layers, and wavelength-independent nonlinear susceptibility [296] could be used for various applications (optical imaging, for example).

Graphene transistors and electronics applications

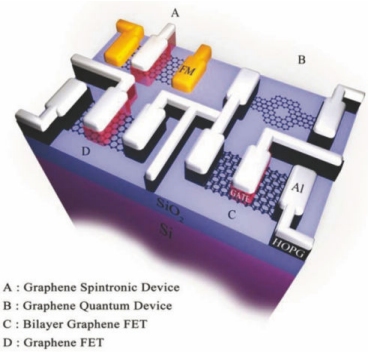

Fig. 25 > A futuristic graphene integrated circuit (not to scale), wherein the desirable properties of various thicknesses of graphene layers are utilized along with strategic oxides (SiO_2, ferroelectric, ferromagnetic, multiferroic, etc.) in response to various external stimuli, such as electric or magnetic fields. In the present illustration, the device structure is fabricated from a very thin single-crystal graphite sheet after subsequent patterning/selective ablation. The remaining graphite acts as a good ohmic contact and interconnection between the top Al metallization (which also acts as a self-aligned mask, protecting the underlying graphite) and the variable-thickness graphene-based devices. Extract from [297]./

Figure 25 shows an artist drawing of a future graphene integrated circuit, in which, after initial wafer scale integration, further lithography, chemical treatments, would be used to engineer active and passive electronic, phononic or spintronics components. This illustrates graphene as a suitable platform to crosslink the nanoscale to conventional microelectronics.

One can envision integrating on the same chip advanced functionalities including chemical sensing, nano-electromechanical resonators, thermal management, and electronic functions. Spintronics will also offer a co-integration of memory and computation functions on the same substrate.

This section overviews the current status of graphene transistors as potential supplement to CMOS technology.

Band gap opening in graphene

Creating a band gap in graphene is one of the major challenges for employing graphene in conventional device circuits, both for analog and digital applications. For digital applications a band gap is mandatory as on/off ratios larger 10^4 are required [298]. For analog applications however, a band gap is not required *per-se*, but the lack of drain current saturation in graphene based FETs and the resulting low voltage gain are major obstacles. A small band-gap~100meV would improve the situation.

Macroscopic graphene field effect transistors

The most straightforward device application of graphene may seem to be as a replacement channel material for silicon MOSFETs. Fig. 26a shows a schematic of such a graphene FET, including a top gate electrode, gate dielectric and source and drain metal contacts. Fig. 26b shows a top view optical micrograph of a macroscopic graphene FET on SiO_2 [299]. The fabrication of graphene FETs follows standard Si process technology once the graphene is deposited and identified. This includes the use of photo- or e-beam lithography, reactive ion etching and thin film deposition for the gate insulators and contacts. Details of typical fabrication processes are described in Refs. [300,301,302].

The transfer characteristics (here: drain current Id vs. back gate voltage V_{bg}) of a typical graphene transistor is shown in Fig. 27. It reveals a major drawback of macroscopic graphene MOSFETs: the absence of a band gap severely limits the current modulation in the graphene FET and, in addition, leads to ambipolar behaviour.

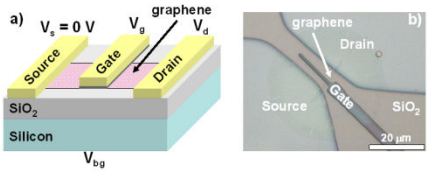

Fig. 26 > a) Schematic cross section and b) optical top-view micrograph of a graphene field effect transistor [299]./

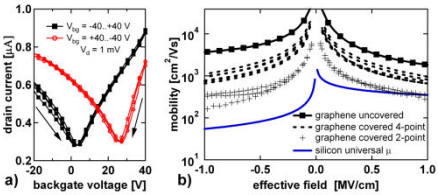

Fig. 27 > a) Drain current versus back gate voltage of a graphene FET. The change of the sweep direction results in considerable hysteresis of 22 V. b) Mobility versus electric field in graphene FETs. Covering graphene with a gate insulator leads to mobility reduction. Contacts have a considerable influence on graphene FETs [299]. Universal mobility of silicon included as reference after Takagi [303]./

The best current modulation reported to date has been about 40, measured at room temperature for water gated graphene [95]. Furthermore, in conjunction with randomly distributed oxide charges the zero band gap leads to a finite minimum charge density even without any applied gate voltage [304]. Consequently, macroscopic graphene transistors conduct substantial current even at their point of minimum conductance (also referred to as Dirac point or charge neutrality point), preventing their application as Si MOSFET replacement. Fig. 27a further shows hysteresis as the gate voltage is swept from negative to positive and vice versa. This typical behaviour occurs despite measuring in vacuum conditions ($P=5x10^{-3}$ mbar) and is a strong indicator of charge traps near the graphene/insulator interface. While suspended graphene measured in ultra high vacuum has been shown to have mobilities exceeding

1000000 cm^2/Vs [20], realistic graphene FETs are limited by substrates and top gates.

Nonetheless, the mobilities in top gated devices exceed those of Si and are typically on the order of several hundred to a thousand cm^2/Vs, even though graphene/ insulator interfaces have not at all been optimized yet [299,300,301,302,305,306]. Fig. 27b shows electron and hole mobilities extracted from several top gated devices, both in 2-point and by 4-point probe configuration.

Graphene nanoribbon transistors

A potential method to create a band gap in graphene is to cut it into narrow ribbons of less than a few tens of nanometers.

GNRs can be armchair or zig-zag edge terminated. In armchair GNRs, the transition from 2D graphene to 1D GNRs leads to quantum confinement and a bandgap that is roughly inversely proportional to the GNR width ($E_g \sim 1/W$) [307,308]. The precise value of the band gap is further predicted to depend on the number N of carbon atoms across the ribbon [307,308,309,310]. This is demonstrated in Fig. 28a, where the simulated density of states (DOS) versus energy for three different hydrogen-terminated armchair GNRs with N = 11, 12 and 13 is shown [14,311].

While the GNR with N = 11 is semi-metallic, the ribbons with 12 and 13 atoms are semiconducting (generally armchair ribbons are semi-metallic at N = 3m− 1, where m is an integer [312]). In hydrogen-terminated zig-zag GNRs, however, the situation is more complicated. Ref. [307] predicted that localized edge states near the Fermi level lead to semi-metallic behaviour, regardless of the number of carbon atoms. On the other hand, Ref. 309 calculated *ab initio* that edge magnetization causes a staggered sublattice potential on the graphene lattice that induces a band gap. Finally, GNRs with other chiral orientation have been considered, including a mix of edges along a ribbon, adding to the complexity of this option [313,314,315,316,317,318,319]. In summary, the simulated results for any form of GNRs should be regarded with care, as they typically share an optimistic assumption of well controlled termination of dangling bonds. In reality, there is likely a great variety of chemical groups terminating the GNR edges. A first detailed discussion has been recently published to address these issues [320], but it is probably reasonable to consider the nature of “real life” zig-zag GNRs still an open question. The predicted presence of a band gap in specific GNRs has been experimentally confirmed.

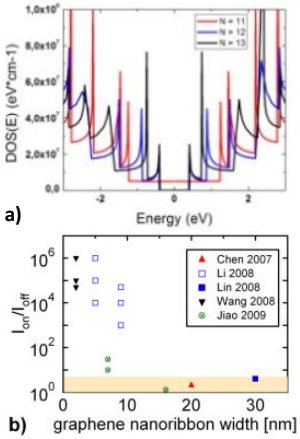

Fig. 28 > a) Simulated DOS vs. energy of hydrogen terminated armchair GNRs for various numbers of electrons N across the ribbon [14]. b) Experimental Ion/Ioff ratios versus GNR width taken from literature. None of the GNRs thus far has shown metallic behavior. The lower colored part of the graph indicates I_{on}/I_{off} values of typical macroscopic graphene FETs; From [14]./

First evidence was reported by Refs.[321,322], where GNRs were structured by e-beam lithography and etched in oxygen plasma with minimum widths~20 nm. The band gaps of these GNRs where in the range of ~30 meV and resulted in field effect transistors with I_{on}/I_{off} ratios of about 3 orders of magnitude at low temperatures (1.7–4 K), reduced to~ 10 at room temperature. These investigations support theoretical predictions that sub-10 nm GNRs are required for true field effect transistor action at room temperature. More importantly, the

experiments revealed a band gap regardless of the chiral orientation of the GNRs [321]. This latter result was attributed to a strong influence of edge states [319,321,323], which dominate over the chirality of the band structure. To date, two examples of sub-10 nm GNRs have been shown experimentally. Ref. 324 fabricated GNRs with a minimum width~1 nm and a band gap of about 500meV using e-beam lithography and repeated, careful over-etching. The resulting transistors consequently switched off at room temperature to "no measurable conductance" [324]. An alternative fabrication process for GNRs was presented by Ref. [109]. Here, GNRs were solution derived from graphite by thermal exfoliation, ultrasonication and ultracentrifugation. The resulting dispersions were deposited onto substrates and GNRs were identified with AFM. The devices exhibited well behaved transistor action at room temperature with $I_{on}/I_{off}>10^6$ [109,325].

The experimental I_{on}/I_{off} ratios reported to date are summarized in Fig. 28b. While they clearly support theoretical predictions and show promise for GNR electronics, they also show an urgent need for further research in this field: Statistical data is scarce and the discrepancies between theory and experiment need to be addressed. The necessity of controllable sub-10nm feature sizes and great uncertainties in chirality control as well as edge state definition remain tremendous challenges. To this end, a recently developed technique, helium ion beam microscopy, has been shown to have potential for precise nano-patterning [326,327].

Bilayer graphene

Another viable approach to obtain a band gap in graphene is to break its symmetry. Ref. [328] proposed that macroscopic BLG would display a suitable band gap if a transverse electric field was applied to break the layer symmetry. Ref. [328] predicts a roughly linear dependence of the gap on applied displacement field, with each 0.1V/nm adding~10meV and a subsequent saturation at about 300meV.

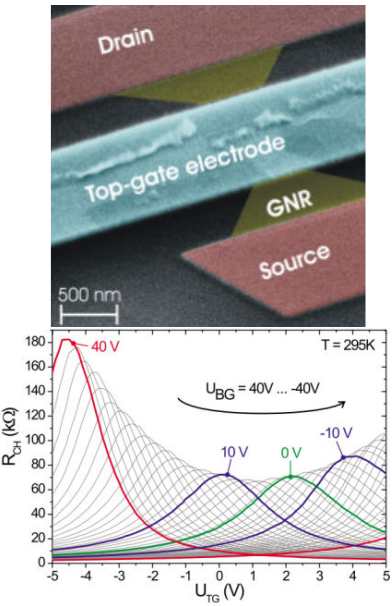

Fig. 29 > Top.SEM image (false color) of a double-gated bilayer graphene FET [333]. Bottom:Channel Resistance of a double-gated bilayer FET as a function of the applied top-gate voltage for different back-gate voltages [333]./

This prediction was experimentally confirmed by Ref. 329 for BLG on SiC through angle-resolved photoemission spectroscopy (ARPES). In their work, they used potassium doping to modify the carrier density, which lead to changes in the electronic band gap [329]. The size of the created band gap was also confirmed by means of infrared spectroscopy [330,331].Ref. [332] took this approach a step further by applying an electrostatic field through a double gate configuration with individually controlled back and top-gate electrodes. However the band gap in their devices could not be utilized to increase the on/off ratio at room temperature due to the presence of intergap states [332]. Only at low temperatures they observed an insulating behaviour in BLG with a perpendicular applied electric displacement field. By optimizing the process technology Refs [258,333] reduced the intergap states in BLG-FETs significantly so that they were able to increase the on/off ratio up~100 at room

temperature by applying an electrical displacement field. This is comparable to the on/off ratio in small band-gap III/V transistors and sufficient for most analog applications. The channel resistance of a double-gated BLG FET is depicted in Fig. 29 [333].

In this device the resistance modulation is 8 at zero applied back-gate and increases to 80 at an applied back-gate of 40V. However, using a double gate structure, with two individually controlled gates, increases complexity, which is not desired in applications. Recently it has been shown that the static gate can be replaced by adsorbate doping [334]. In this work a band gap could be obtained and utilized to increase the on/off ratio with only one gate electrode [334].

Using BLG with a perpendicular electric field Ref.335 realized logic gates. By combining a p-type and an n-type BLG FET with an induced band gap, Ref. 335 realized NAND and NOR gates, fundamental building blocks for digital logic circuits. The operation of NOR gates and the resulting operation of the BLG based NOR gate are depicted in Fig. 30

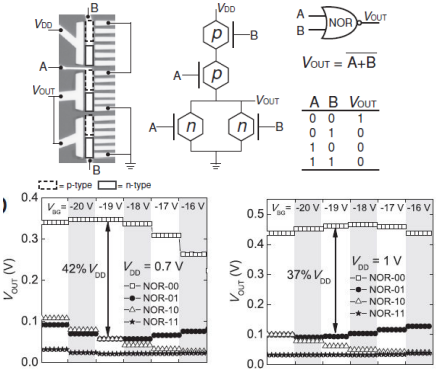

Fig. 30 >Top: Device wiring used for realizing a NOR gate; corresponding circuit diagram and the truth table of the operation (taken from [194]). Bottom: The operation at a drive voltage 0.7 V and 1.0 V, respectively (taken from [335])./

Summary band gap engineering in graphene

Over the past few years different approaches were explored for creating a band gap in graphene, whereof confinement to GNRs and BLG are the most promising. Using graphene in switches for digital operation requires a band gap>400meV, hence confining graphene to GNRs is necessary. Using bottom-up synthesis on/off ratios larger 10^6 are achievable using GNRs [325].

The challenges is to develop industrially compatible top-down methods for the fabrication of such small structures. In contrast, in BLGs a band gap could be realized using standard top-down fabrication, but as the theoretical limits of the band gap in BLG are~300 meV an application to digital circuits will be challenging. However analog applications can strongly benefit from this band gap, which is tuneable by electric means.

RF Transistors

Numerous communication systems rely on electromechanical devices, such as filters, resonators, and RF switches. Their miniaturization will strongly affect the development of future communication systems. The ultimate limit to this miniaturization is represented by graphene electromechanical devices.

Graphene combines exceptional electronic properties with excellent mechanical properties. Its ambipolar transport properties, ultra thin and flexible, and electrostatic doping offer a new degree of freedom for the development of advanced electronic devices with many potential applications in communications and RF electronics.

For RF analog applications a high on-off ratio is desirable but not mandatory. Instead, most relevant for good RF performance is a FET channel with excellent carrier transport properties (high mobility and maximum velocity) [336], combined with a small scale length, which improves strongly as the channel material thickness is reduced [337]. Graphene RF FETs have been investigated, both using exfoliated [306,338] and epitaxial materials [339,340]. Graphene transistors with a 240nm

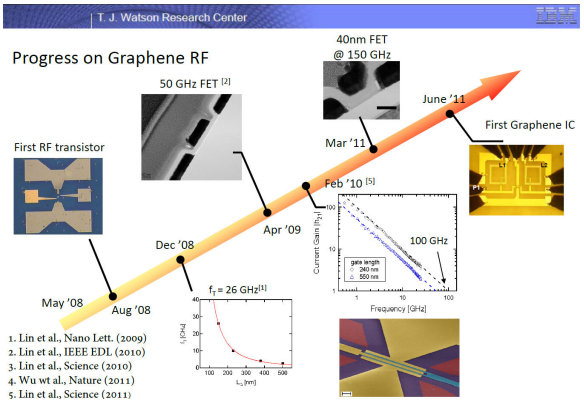

Fig. 31 > Summary of published graphene RF transistor data (Courtesy of Yu Min Lin, IBM, USA)./

gate operating at frequencies up to 100 GHz were demonstrated in early 2010 [341]. This cut-off frequency is already higher than those achieved with the best silicon MOSFET having similar gate lengths [342].

Higher f_T can be expected for optimized devices with shorter gate lengths as demonstrated by the progress achieved by the IBM group that in 2 years improved the performances of their Graphene-based RF transistor passing from 26 GHz[306] to 155 GHz[343] (Fig. 31). The latter result was achieved with CVD graphene was grown on copper film and transferred to a wafer of diamond-like carbon. This once more emphasizes the need for graphene/insulator interface engineering.

Cut-off frequency over 300 GHz were demonstrated with a 140 nm channel length [344], comparable with the very top high-electron-mobility transistors (HEMTs) with similar gate length [345], see Fig.32. These results are impressive, considering that RF graphene research has been done for a fraction of the time devoted thus far to conventional devices. As shown in Fig. 32, the progress in graphene-based high frequency devices has been impressive. This progress opens new horizons for quick development of plethora of applications in RF communications.

Compared to conventional Si and III-V materials, ambipolar graphene electronics has many advantages. The higher mobility allows higher operating frequencies for frequency doubling and mixing. In addition, ambipolar devices can significantly reduce the number of transistors needed. Simpler circuits mean less power consumption and smaller chip area. Graphene is also an ideal material for flexible electronics integration.

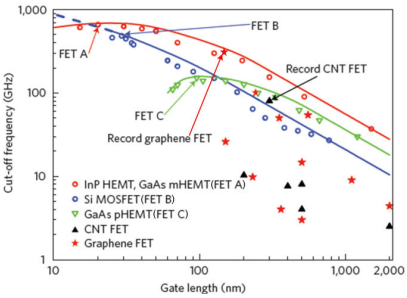

Fig. 32 >Comparing cut-off frequency versus gate length for graphene MOSFETs, nanotube FETs and three types of radiofrequency FET (Adapted from ref.321). /

To take advantage of the full potential of graphene devices, basic research needs to be combined with improved material growth and device technology. A better understanding of parameters such as breakdown voltage, electron velocity, and saturation current is needed to allow a complete benchmark and evaluation of this material. Once the growth and fabrication technology of these new devices matures, their integration with conventional Si electronics, and/or flexible and transparent substrates has the potential to transform communications. Thus graphene can be seen, rather than as a replacement of Si technology, as a complement to it in a "More than Moore"[346] perspective.

Non-conventional graphene switches

A number of concepts for (non-volatile) graphene switches have emerged based on mechanisms other than the classic field effect. Even though a thorough review is beyond the scope of this leaflet, they are briefly introduced in this section. A first concept are graphene/GO Schottky barrier MOSFETs [347], where semiconducting GO acts as the transistor channel. Another approach relies on creating nanoscale gaps by electric fields [348]. These are reversibly opened and closed by breaking and re-forming the carbon atomic chains [348].

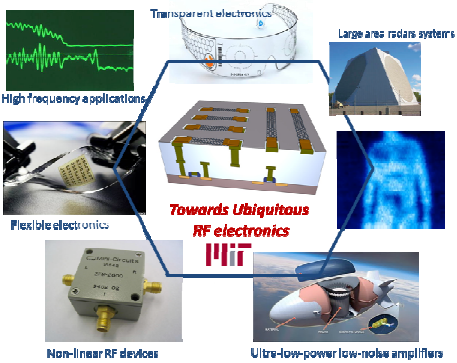

Fig. 33 > Possible applications of graphene RF transistor (Courtesy of Tomas Palacios, MIT, USA)./

Chemical surface modification affects strongly the electronic band structure of graphene [349]. The electrostatical control of drain current can be reversibly modified in a graphene FET by controlled chemisorption [350]. Ferroelectric gating has been shown to electrostatically dope graphene and change the drain currents in a non-volatile way [351]. While these early concepts are far from mature, they nevertheless demonstrate the potential of graphene for nanoelectronics applications that might not be anticipated today.

Atomistic simulations of transistors

Due to the novelty of the graphene research field, device design principles have not yet been extensively elaborated, and different design options must be explored, evaluated and optimized. From this perspective, numerical simulations can greatly help.

When dealing with the investigation of device electrical behaviour, atomistic features of the material, such as for example the lattice potential, disappear behind a series of synthetic parameters like the effective mass tensor. The price to pay is however the lack of accuracy at the atomic level, which can be obtained through *ab-initio* simulations, at the expense of huge computational requirements, especially when the number of atoms is of the order of few thousands like in realistic FETs.

The strategy is then to find a trade-off, leveraging on atomistic simulations based on the Non-Equilibrium Green's Function (NEGF) formalism, which can provide physical insight at the atomic level, but with fewer computational burden as compared to DFT calculations.

Efforts towards the understanding of BLG for next-generation devices have been first addressed in [352], where a double gate FET was simulated by means of the self-consistent solution of the 2D Poisson and Schrödinger equation with open-boundary conditions, within NEGF. Strong band-to-band tunnelling heavily limits device performance, since the current in the off-state is too large for digital applications, when applying drain-to-source voltages complying with the International Technology Roadmap for Semiconductors (ITRS) [298], i.e. approximately 0.5 V.

The large tunnelling component, instead of being detrimental like in thermionic devices, can be turned into an advantage in tunnel FETs [353], whose main appeal is represented by a sub-threshold swing well below those achievable in thermionic devices (<60mV/dec)[354]. This would allow reducing the supply voltage for digital logic applications, and consequently the power consumption. It is indeed well known that power dissipation is nowadays the most limiting factor in integrated circuits, so that all future approaches need be directed towards the design of low power devices, the so-called "Green Transistors"[355]. From this perspective, BLG

tunnel FET (see Fig.34) represents a viable option, because of its large I_{on}/I_{off} ratios (large than 10^3), even when applying ultra-low power supply (0.1 V) [353]. An alternative FET, based on graphene heterostructures with atomically thin boron nitride acting as a tunnel barrier, was recently demonstrated [356].

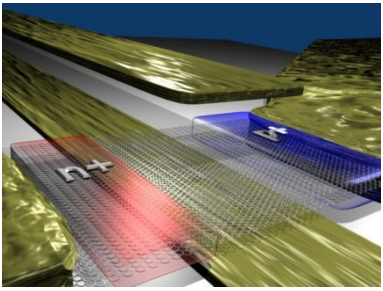

Fig. 34 > Sketch of the bilayer graphene tunnel FET proposed in [353]./

The operation of the device (see Fig. 35) relies on the voltage tunability of the tunnelling density of states and of the effective height of the tunnel barrier adjacent to the graphene electrode [356]. The device exhibits room temperature switching ratios of ~50. However, this value can be improved by optimizing the device structure and up to 10^5 was recently reported by using MoS_2 instead of BN [357].

Lateral confinement, as in GNRs, is another approach widely addressed in the last year to induce an energy gap. Simulations have provided relevant information regarding the potential and the limits of this approach [358,359]. In particular, GNRs smaller than 3 nm are needed to comply with ITRS, which is very difficult to achieve with state-of-the-art electron beam lithography [360]. Things get even worse when considering sources of non-idealities, such as line-edge roughness or single vacancy defects, which strongly limit electron mobility in GNRs, another important figure of merit for digital applications [361]. However, even when dealing with perfect edges, mobility in narrow devices (W<2nm) is strongly limited by electron-phonon coupling, leading to similar mobility as the Si counterpart [362].

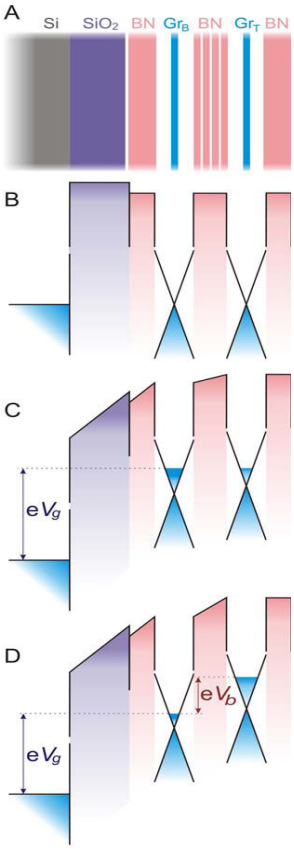

Fig. 35 > (a) Schematic structure of the graphene heterostructure FET. The corresponding band structure with (b) no gate voltage and (c) finite gate voltage V_g and zero bias V_b applied. (d) Band structure when both Vg and V_b are finite. The cones illustrate graphene's Dirac-like spectrum and, for simplicity, the tunnel barrier for electrons is considered [adapted from ref. 322]./

Chemical functionalization is a viable route toward bandgap engineering. Ref. [363] exposed graphene to a stream of hydrogen atoms leading to a material close to the ideal graphane. DFT suggests that [364] graphane would have a 5.4 eV gap, while it reduces to 3.2 eV in 50% hydrogenated graphene. A recent study (Fig. 36) [365] suggested that such devices can provide large currents as well as I_{on}/I_{off} ratios, and can represent a promising option for future technology nodes.

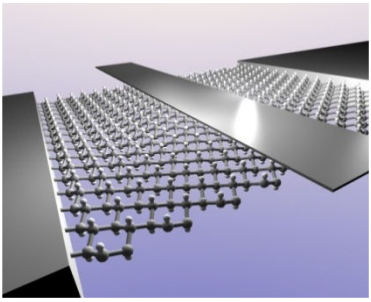

Fig. 36 > Sketch of the functionalized graphene based transistor./

Probably more than towards digital applications, research should be focus on analog electronics, where the lack of a bandgap does not represent an issue, and high performance in terms of cutoff frequency in RF applications can be achieved [366], and negative differential resistance [367,368] can be exploited in a range of applications, such as oscillators, fast switching logic, and low power amplifiers.

Conclusion

Graphene has already demonstrated high potential to impact most areas of electronic information technology, ranging from top end high performance applications in ultrafast information processing, to consumer applications using transparent or flexible electronic structures. This is testified by the increasing number of chip-makers now active in graphene research.

The combination of its unique optical and electronic properties, in addition to flexibility, robustness and environmental stability, make graphene an extremely interesting material for future photonic and optoelectronic devices.

Graphene can successfully replace many materials (*i.e.* ITO) in several existing applications, but certainly, the combination of its unique properties will inspire completely new applications and is where future research should focus (i.e. creating new technologies exploiting the uniqueness of graphene and related inorganic 2d crystals, rather than just try to displace existing and established technologies).

Graphene may allow high-speed, compact-footprint electro-optical modulators, switches and photodetectors integrated with waveguides or plasmonic circuits. Moreover, the mechanical flexibility of graphene will also enable integration with bendable substrates and plastic waveguides.

Graphene can detect light beyond the current limit set by the band gap of traditional semiconductors, opening new applications in the far-infrared (terahertz, THz) and mid-infrared regimes (e.g. bolometers and cameras), and provides the potential for ultrafast pixelated detection with ballistic transport of generated *n*. This could enable portable terahertz sensors for remote detection of dangerous agents, environmental monitoring or wireless communication links with transmission rates above 100 Gbit/s. Moreover, it can be exploited for photocurrent generation by providing a gain mechanism where multiple carriers are created from one incident photon.

The compatibility of graphene with standard CMOS processes at wafer scale makes it a promising candidate for future electronics, particularly for high data-rate (inter- and intra-chip) interconnects. While macroscopic graphene transistors are not suitable for logic applications, due to the lack of band gap, graphene RF transistors seem promising and feasible. Graphene nanoribbons, on the other hand, show promise as a CMOS compatible approach, but their extreme sensitivity at an atomic level to both geometric and edge termination variations may well render their practical use extremely challenging. Non-classic switching mechanisms may eventually lead to a co-integration of graphene into silicon technology, even though details are not yet clear today. In addition to these device related issues, there is the imperative need of a large area, CMOS compatible deposition or placement technique. As CVD and related methods are being explored, many device

related questions are being addressed using the existing manufacturing methods. These insights will be transferable as soon as industrially relevant production and placement technologies will become available.

Acknowledgment

CPE thanks COST MP0901 "NanoTP" for support, as well as ANR NANOSIM-GRAPHENE. JC acknowledges financial support from the Alexander von Humboldt Foundation, the French ANR (NMGEM project) and the EC (GRENADA project). A. C. F. acknowledges funding from EU grants GRAPHENE-CA, NANOPOTS, GENIUS, RODIN, EPSRC grants EP/GO30480/1 and EP/F00897X/1, and a Royal Society Wofson Research Merit Award. FB and ACF acknowledge Paul Beecher, Tawfique Hasan, Zoran Radivojevic and Zhipei Sun for useful discussion.

References

[1] Novoselov, K. S., Castro Neto, A. *New directions in science and technology: two-dimensional crystals* Rep. Prog. Phys. 74 082501 (2011)

[2] Bae, S. *et al. Roll-to-roll production of 30-inch graphene films for transparent electrodes* Nature Nanotech. 5, 1 (2010).

[3] http://www.nobelprize.org/nobel_prizes/physics/laureates/2010/press.html.

[4] Lin, Y-M et al., Wafer-Scale Graphene Integrated Circuit Science 332, 1294 (2011).

[5] http://research.nokia.com/morph

[6] Torrisi, F., *et al., Ink-Jet Printed Graphene Electronics.* arXiv:1111.4970v1 (2011).

[7] Hernandez, Y., *et al. High-yield production of graphene by liquid-phase exfoliation of graphite*. Nature Nanotech. 3, 563 (2008).

[8] Tannock, Q., *Exploiting carbon flatland*, Nat. Mater. 11, 2 (2012).

[9] Harrison, W.A., ed. Electronic Structure and Properties of Solids: *the Physics of the Chemical Bond*. 1989, Dover Publications.

[10] Charlier, J.C., et al. *Electron and phonon properties of graphene: Their relationship with carbon nanotubes* Topics. Appl. Physics 111, 673 (2008).

[11] Wallace, P. R., *The Band Theory of Graphite* Phys. Rev. 71, 622 (1947).

[12] Geim, A.K. and K.S. Novoselov, *The rise of graphene.* Nature Mater.6, 183 (2007).

[13] Ando, T., *The electronic properties of graphene and carbon nanotubes.* NPG Asia Mater. 1, 17 (2009).

[14] Lemme M., *Current status in graphene transistors.* Solid State Phenom., 499 156 (2010).

[15] Novoselov, K.S., et al., *Two-dimensional gas of massless Dirac fermions in graphene.* Nature 438, 197 (2005).

[16] Berger, C., *et al.*, *Electronic confinement and coherence in patterned epitaxial graphene.* Science, 312 1191 (2006).

[17] Bolotin, K.I., *et al.*, *Ultrahigh electron mobility in suspended graphene.* Solid State Communications 146, 351 (2008).

[18] Morozov, S.V., *et al., Giant Intrinsic Carrier Mobilities in Graphene and Its Bilayer.* Phys. Rev. Lett., 100, 016602 (2008).

[19] Du, X., *et al., Approaching ballistic transport in suspended graphene.* Nature Nanotech. 3, 491 (2008).

[20] Castro, E. V., *et al., Limits on Charge Carrier Mobility in Suspended Graphene due to Flexural Phonons.* Phys. Rev. Lett. 105, 266601 (2010).

[21] Moser, J., Barreiro, A., Bachtold, A. *Current-induced cleaning of graphene. Appl. Phys. Lett.* 91, 163513 (2007).

[22] Balandin, A.A., *et al.*, *Superior Thermal Conductivity of Single-Layer Graphene.* Nano Lett. 8, 902 (2008).

[23] Ghosh, S., *et al., Extremely high thermal conductivity of graphene: Prospects for thermal management applications in nanoelectronic circuits.* Appl. Phys. Lett. 92, 151911 (2008).

[24] Nair, R. R., *et al. Fine structure constant defi nes transparency of graphene.* Science 320, 1308 (2008).

[25] Lee, C., *et al.* Measurement of the Elastic Properties and Intrinsic Strength of Monolayer Graphene Science 321, 385, (2008).

[26] Booth, T.J., *et al., Macroscopic Graphene Membranes and Their Extraordinary Stiffness.* Nano Letters 8, 2442 (2008).

[27] Baughman, R. H., Zakhidov, A. A., de Heer, W. A. *Carbon Nanotubes—the Route Toward Applications* Science 297, 787 (2002).

[28] Cai, J., P. *et al*., *Atomically precise bottom-up fabrication of graphene nanoribbons* Nature 466, 470 (2010).

[29] Brodie, B.C., *Sur le poids atomique du graphite Ann*. Chim. Phys., 55, 466 (1860).

[30] Hummers, W.S. and R.E. Offeman, *Preparation of graphite oxide* J. Am. Chem. Soc. 80, 1339 (1958).

[31] Staudenmaier, L., Ber. Deut. Chem. Ges., 31, 1481 (1898).

[32] Titelman, G. I., *et al. Characteristics and microstructure of aqueous colloidal dispersions of graphite oxide* Carbon 43, 641 (2005).

[33] Liscio, A., *et al., Charge transport in graphene–polythiophene blends as studied by Kelvin Probe Force Microscopy and transistor characterization* J. Mater. Chem. 21, 2924 (2011).

[34] Quintana, M., A., *et al., Selective organic functionalization of graphene bulk or graphene edges* Chem. Comm. 47, 9330 (2011).

[35] Melucci, M., E. et al., *Facile covalent functionalization of graphene oxide using microwaves: bottom-up development of functional graphitic materials* J. Mater. Chem., 20, 9052 (2010).

[36] Matsuo, Y., *et al. Silylation of graphite oxide*, Carbon, 42, 2117 (*2004).*

[37] Englert, J.M., *et al. Covalent bulk functionalization of graphene* Nature Chem. 3, 279 (2011).

[38] Backes, C., *et al., Nanotube surfactant design: the versatility of water-soluble perylene bisimides.* Adv. Mater., 22, 788 (2010).

[39] Wang, Q.H. and Hersam, M.C. *Room-temperature molecular-resolution characterization of self-assembled organic monolayers on epitaxial graphene.* Nature Chem. 1, 206 (2009).

[40] Mattevi, C. *et al. Evolution of electrical, chemical, and structural properties of transparent and conducting chemically derived graphene thin films.* Adv. Funct. Mater. 19, 2577 (2009).

[41] Erickson, K., R. *et al., Determination of the local chemical structure of graphene oxide and reduced graphene oxide* Adv. Mater, 22, 4467 (2010).

[42] Eda, G., Chhowalla, M., *Chemically Derived Graphene Oxide: Towards Large-Area Thin-Film Electronics and Optoelectronics.* Adv. Mater. 22, 2392 (2010).

[43] Treossi, E., M. *et al., High-contrast visualization of graphene oxide on dye-sensitized glass, quartz and silicon by fluorescence quenching* J. Am. Chem. Soc., 131, 15576 (2009).

[44] Becerril, H.A., *et al., Evaluation of solution-processed reduced graphene oxide films as transparent conductors.* ACS Nano, 2, 463 (2008).

[45] Stankovich, S., *et al., Synthesis of graphene-based nanosheets via chemical reduction of exfoliated graphite oxide.* Carbon, 2007, 45, 1558-1565.

[46] Gilje, S., *et al., A chemical route to graphene for device applications.* Nano Lett., 7, 3394 (2007).

[47] Zhou, M., *et al., Electrochemically Reduced Graphene Oxide Films.* Chemistry-a European Journal, 15, 6116 (2009).

[48] Yao, P.P., *et al., Electric Current Induced Reduction of Graphene Oxide and Its Application as Gap Electrodes in Organic Photoswitching Devices.* Adv. Mater. 22, 5008 (2010).

[49] Bagri, A., *et al., Structural evolution during the reduction of chemically derived graphene oxide ,* Nature Chem. 2, 581 (2010).

[50] Pang, S.P., *et al. Patterned Graphene Electrodes from Solution-Processed Graphite Oxide Films for Organic Field-Effect Transistors* Adv. Mater. 21, 3488 (2009,).

[51] Eda, G. and Chhowalla, M. *Graphene-based Composite Thin Films for Electronics.* Nano Letters, 9, 814 (2009).

[52] Wu, J.B., *et al., Organic solar cells with solution-processed graphene transparent electrodes.* Appl. Phys. Lett. 92, 263302 (2008).

[53] Yang, N.L., *et al., TiO2 Nanocrystals Grown on Graphene as Advanced Photocatalytic Hybrid Materials.* ACS Nano, 4, 887 (2010).

[54] Zhu, X.J., *et al., Nanostructured reduced graphene oxide/Fe2O3 composite as a high-performance anode material for lithium ion batteries.* ACS Nano, 5, 3333 (2011)

[55] Wei, Z.Q., *et al., Nanoscale Tunable Reduction of Graphene Oxide for Graphene Electronics.* Science, 328, 1373 (2010).

[56 Alaboson, J.M.P., *et al., Conductive Atomic Force Microscope Nanopatterning of Epitaxial Graphene on SiC(0001) in Ambient Conditions.* Adv. Mater., 23, 2181 (2011).

[57] Mativetsky, J.M., *et al., Local Current Mapping and Patterning of Reduced Graphene Oxide.* J. Am. Chem. Soc., 132, 14130 (2010).

[58]He, S. J., *et al., A Graphene Nanoprobe for Rapid, Sensitive, and Multicolor Fluorescent DNA Analysis.* Adv. Funct. Mater. 20, 453 (2010).

[59] Merchant, C. A., *et al., DNA Translocation through Graphene Nanopores.* Nano Lett. 10, 2915 (2010).

[60] Schneider, G.F., *et al., DNA Translocation through Graphene Nanopores*, Nano Lett. 10, 3163 (2010).

[61] Rochefort, A. and Wuest, J.D. Interaction of Substituted Aromatic Compounds with Graphene Langmuir, 2009, 25, 210-215.

[62] Roos, M., *et al., Hierarchical Interactions and Their Influence upon the Adsorption of Organic Molecules on a Graphene Film*. J. Am. Chem. Soc. 133, 9208 (2011).

[63 Gierz, I., *et al. Atomic Hole Doping of Graphene*. Nano Lett. 8, 4603 (2008).

[64] Wehling, T.O., *et al., Molecular doping of graphene.* Nano Lett. 8, 173 (2008).

[65] Lauffer, P., *et al., Molecular and electronic structure of PTCDA on bilayer graphene on SiC(0001) studied with scanning tunneling microscopy.* Phys. Stat. Solidi B-Basic Solid State Physics 245, 2064 (2008).

[66 Zhang, Y.H., *et al. Tuning the electronic structure and transport properties of graphene by noncovalent functionalization: effects of organic donor, acceptor and metal atoms*. Nanotechnology 21, (2010).

[67] Matte, H., *et al., Quenching of fluorescence of aromatic molecules by graphene due to electron transfer*. Chem. Phys. Lett., 506, 260 (2011).

[68] Swathi, R. S. and Sebastiana K. L. *Resonance energy transfer from a dye molecule to graphene* J. Chem. Phys. 129, 054703 (2008).

[69] Treossi, E., *et al., High-Contrast Visualization of Graphene Oxide on Dye-Sensitized Glass, Quartz, and Silicon by Fluorescence Quenching*. J. Am. Chem. Soc. 131, 15576 (2009).

[70] Wang, Y.B., *et al., Fluorescence Quenching in Conjugated Polymers Blended with Reduced Graphitic Oxide.* J. Phys. Chem. C, , 114, 4153 (2010).

[71 Kim, J., *et al. Graphene Oxide Sheets at Interfaces.* J. Am. Chem. Soc. 132, 260 (2010).

[72] Loh, K.P., *et al., Graphene oxide as a chemically tunable platform for optical applications.* Nature Chem. 2, 1015 (2010).

[73] Rao, C.N.R. and Voggu, R. *Charge-transfer with graphene and nanotubes.* Materials Today 13, 34 (2010).

[74] Novoselov, K.S., *et al., Electric Field Effect in Atomically Thin Carbon Films.* Science 306, 666 (2004).

[75] Casiraghi, C., *et al., Rayleigh Imaging of Graphene and Graphene Layers.* Nano Lett. 7, 2711 (2007).

[76] Blake, P., *et al., Making graphene visible.* Appl. Phys. Lett. 91, 063124 (2007.).

[77] Abergel, D.S.L., A. Russell, and V.I. Fal'ko, *Visibility of graphene flakes on a dielectric substrate.* Appl. Phys. Lett. 91, 063125 (2007).

[78] Ni, Z.H., *et al., Graphene Thickness Determination Using Reflection and Contrast Spectroscopy.* Nano Lett. 7, 2758 (2007).

[79] Ferrari, A.C., *et al., Raman Spectrum of Graphene and Graphene Layers.* Phys. Rev.Lett. 97, 187401 (2006).

[80] Ferrari, A.C., *Raman spectroscopy of graphene and graphite: Disorder, electron-phonon coupling, doping and nonadiabatic effects.* Solid State Comm. 143, 47 (2007).

[81] Tuinstra, F. and Koenig, J. L. *Raman Spectrum of Graphite* J. Chem. Phys. 53, 1126 (1970).

[82] Ferrari, A.C. and Robertson, J., *Raman of amorphous, nanostructured, diamond-like carbon and nano-diamond*. Philos. Trans. R. Soc. Ser. A 362, 2477 (2004).

[83] J. Yan, *et al.*, *Electric Field Effect Tuning of Electron-Phonon Coupling in Graphene*. Phys. Rev. Lett. 98, 166802 (2007).

[84] *Ando, T. , Magnetic Oscillation of Optical Phonon in Graphene J. Phys. Soc. Jpn. 76, 024712* (2007).

[85] Goerbig, M.O. *et al., Filling-Factor-Dependent Magnetophonon Resonance in Graphene* Phys. Rev. Lett. 99, 087402 (2007).

[86] Basko, D.M., et al., *Electron-electron interactions and doping dependence of the two-phonon Raman intensity in graphene.* Phys. Rev. B 80, 165413 (2009).

[87] Das, A., et al., *Monitoring dopants by Raman scattering in an electrochemically top-gated graphene transistor.* Nature Nanotechnology 3, 210 - 215 (2008).

[88] Malard, L. M. et al., *Probing the electronic structure of bilayer graphene by Raman scattering.* Phys. Rev. B 76, 201401 (2007).

[89] Pisana, S. et al., *Breakdown of the adiabatic Born–Oppenheimer approximation in graphene.* Nature Mater. 6, 198 (2007).

[90] Yan, J., et al., *Observation of Magnetophonon Resonance of Dirac Fermions in Graphite.* Phys. Rev. Lett. 105, 227401 (2010).

[91] Faugeras, C., et al., *Magneto-Raman Scattering of Graphene on Graphite: Electronic and Phonon Excitations*. Phys. Rev. Lett. 107, 036807(2011).

[92] Mohiuddin, M. G., et al., *Uniaxial strain in graphene by Raman spectroscopy: G peak splitting, Grüneisen parameters, and sample orientation.* Phys. Rev. B 79, 205433 (2009).

[93] Ferralis,N. Maboudian, R. and Carraro, C., *Evidence of Structural Strain in Epitaxial Graphene Layers on 6H-SiC(0001).* Phys. Rev. Lett. 101, 156801 (2008).

[94] Casiraghi, C., et al., *Raman Fingerprint of Charged Impurities in Graphene.* Appl. Phys. Lett. 91, 233108 (2007).

[95] Das, A.,et al., *Monitoring dopants by Raman scattering in an electrochemically top-gated graphene transistor.* Nature Nanotech. 3, 210 (2008).

[96] Casiraghi, C., et al., *Raman spectroscopy of graphene edges.* Nano Lett. 9, 1433 (2009).

[97] Ferrari A. C. et al., *Resonant Raman spectroscopy of disordered, amorphous, and diamondlike carbon.* Phys. Rev. B 64, 075414 (2001).

[98] Lotya, M. et al. *Liquid phase production of graphene by exfoliation of graphite in surfactant/water solutions.* J. Am. Chem. Soc. 131, 3611

[99] Green, A. A. & Hersam, M. C. *Solution phase production of graphene with controlled thickness via density diff erentiation.* Nano Lett. 9, 4031 (2009).

[100] Maragò, O. M., et al., *Brownian motion of graphene.* ACS Nano 4, 7515 (2010).

[101] Hasan, T., *et al. Solution-phase exfoliation of graphite for ultrafast photonics*. Phys. Status Solidi B **247**, 2953 (2010)

[102] Khan, U., *et al. High-Concentration Solvent Exfoliation of Graphene*.Small 6, 864 (2010).

[103] Nuvoli, D. *et al. High concentration few-layer graphene sheets obtained by liquid phase exfoliation of graphite in ionic liquid.* J.Mater. Chem. 21, 3428 (2011).

[104] Bonaccorso F., *et al., Graphene photonics and optoelectronics*. Nature Photon. 4, 611 (2010).

[105] Lee, J. H., *et al., One-Step Exfoliation Synthesis of Easily Soluble Graphite and Transparent Conducting Graphene Sheets.* Adv. Mater. 21, 4383 (2009).

[106] Valles, C., et al., *Solutions of negatively charged graphene sheets and ribbons.* J. Am. Chem. Soc. 130, 15802 (2008).

[107] Li, D. *et al. Processable aqueous dispersions of graphene nanosheets.* Nature Nanotech. 3, 101 (2008).

[108] An, X. *et al. Stable Aqueous Dispersions of Noncovalently Functionalized Graphene from Graphite and their Multifunctional High-Performance Application*s. Nano Lett. 10, 4295 (2010).

[109] Li, X., *et., Chemically Derived, Ultrasmooth Graphene Nanoribbon Semiconductors*. Science 319, 1229 (2008).

[110] Coleman, J. N., *et al. , Two-Dimensional Nanosheets Produced by Liquid Exfoliation of Layered Materials.* Science 331, 568 (2011).

[111] Acheson, E. G., *Production of artifi cial crystalline carbonaceous materials; article of carborundum and process of the manufacture thereof carborundum*. US patent 615,648 (1896).

[112] Berger, C., *et al., Ultrathin epitaxial graphite: 2D electron gas properties and a route toward graphene-based nanoelectronics*. J. Phys. Chem. B 108, 19912 (2004).

[113] Berger, C., *et al., Electronic confinement and coherence in patterned epitaxial graphene*. Science 312, 1191 (2006).

[114] De Heer, W.A., *et al., Epitaxial graphene*. Solid State Communications. 143, 92 (2007).

[115] Emtsev, K. V., *et al., Towards wafer-size graphene layers by atmospheric pressure graphitization of silicon carbide*. Nature Mater. 8, 203 (2009).

[116] Riedl, C. *et al. Quasi-free-standing epitaxial graphene on SiC obtained by hydrogen intercalation*. Phys. Rev. Lett. 103, 246804 (2009).

[117] Kedzierski, J., *et al., Epitaxial Graphene Transistors on SiC Substrates.* Electron Devices, IEEE Transactions. 55, 2078 (2008).

[118] Rohrl, J., *et al., Raman spectra of epitaxial graphene on SiC(0001).* Appl. Phys. Lett. 92, 201918 (2008).

[119] Obraztsov, A. N., *et al., Chemical vapor deposition of thin graphite films of nanometer thickness.* Carbon 45, 2017 (2007).

[120] Yu, Q., *et al., Graphene segregated on Ni surfaces and transferred to insulators.* Appl. Phys. Lett. 93, 113103 (2008).

[121] Reina, A., *et al., Large Area, Few-Layer Graphene Films on Arbitrary Substrates by Chemical Vapor Deposition.* Nano Lett. 9, 30 (2009).

[122] Kim, K.S., *et al., Large-scale pattern growth of graphene films for stretchable transparent electrodes.* Nature 457, 706 (2009).

[123] Sutter, P.W., J.-I. Flege, and E.A. Sutter, *Epitaxial graphene on ruthenium*. Nature Mater. 7, 406 (2008).

[124] Coraux, J., *et al., Structural Coherency of Graphene on Ir(111).* Nano Lett. 8, 565 (2008).

[125] N'Diaye, A.T., *et al., Structure of epitaxial graphene on Ir(111).* New Journal of Physics 10, 043033 (2008).

[126] Li, X., *et al., Large-Area Synthesis of High-Quality and Uniform Graphene Films on Copper Foils*. Science 324, 1312 (2009).

[127] Rummeli, M. H., *et al. Direct Low-Temperature Nanographene CVD Synthesis over a Dielectric Insulator.* ACS nano 4, 4206 (2010).

[128] Hwang, J., *et al., Epitaxial growth of graphitic carbon on C-face SiC and Sapphire by chemical vapor deposition (CVD*). J. Crystal Growth 312, 3219 (2010).

[129] Michon, A. , *et al., Direct growth of few-layer graphene on 6H-SiC and 3C-SiC/Si via propane chemical vapor deposition.* Appl. Phys. Lett. (2010) 97, 171909.

[130] Strupinski, W., *et al., Graphene Epitaxy by Chemical Vapor Deposition on SiC.* Nano Lett. 11, 1786 (2011).

[131] Fanton, M. A., *et al., Characterization of Graphene Films and Transistors Grown on Sapphire by Metal-Free Chemical Vapor Deposition.* ACS Nano 5, 8062 (2011).

[132] Sun, J., *et al., Large-area uniform graphene-like thin films grown by chemical vapor deposition directly on silicon nitride.* Appl. Phys. Lett. 98, 252107 (2011).

[133] Scott, A., *et al., The catalytic potential of high-κ dielectrics for graphene formation*.Appl. Phys. Lett. 98, 073110 (2011).

[134] Dato, A. *et al., Substrate-Free Gas-Phase Synthesis of Graphene Sheets* Nano Lett. 8, 2012 (2008).

[135] Al-Temimy, A., *et al., Low temperature growth of epitaxial graphene on SiC induced by carbon evaporation*. Appl. Phys. Lett. 95, 231907 (2009).

[136] Bertoni, G., *et al., First-principles calculation of the electronic structure and EELS spectra at the graphene/Ni(111) interface*. Phys. Rev. B 71, 075402 (2004)

[137] Land, T. A., *et al., STM investigation of single layer graphite structures produced on Pt(111) by hydrocarbon decomposition* Surf. Sci. 264, 261 (1992).

[138] N'Diaye, A. T., *et al., Two-Dimensional Ir Cluster Lattice on a Graphene Moiré on Ir(111*). Phys. Rev. Lett. 97, 215501 (2006).

[139] Klusek, Z., *et al., Local electronic edge states of graphene layer deposited on Ir(1 1 1) surface studied by STM/CITS.* Appl. Surf. Sci. 252, 1221 (2005).

[140] Marchini, S., Günther, S., Wintterlin, J., *Scanning tunneling microscopy of graphene on Ru(0001).* Phys. Rev. B 76, 075429 (2007).

[141] Vázquez de Parga, A. L., et al., *Periodically Rippled Graphene: Growth and Spatially Resolved Electronic Structure.* Phys. Rev. Lett. 100, 056807 (2007).

[142] Rosei, R., et al., *Structure of graphitic carbon on Ni(111): A surface extended energy-loss fi ne-structure study*. Phys. Rev. B 28, 1161–1164 (1983).

[143] Dedkov, Y. S., Fonin, M., Laubschat, C., *A possible source of spin-polarized electrons: The inert graphene/Ni(111) system*. Appl. Phys. Lett. 92, 052506 (2008).

[144] Dedkov Y. S., *et al., Rashba Effect in the Graphene/Ni(111) System*. Phys. Rev. Lett. 100, 107602 (2008).

[145] Busse, C., *et al., Graphene on Ir(111): Physisorption with Chemical Modulation.* Phys. Rev. Lett., 107, 036101 (2011).

[146] Martoccia, D. , *et al., Graphene on Ru(0001): A 25×25 Supercell*. Phys. Rev. Lett. 101, 126102 (2008).

[147] Blanc, N., *et al*., submitted

[148] Giovannetti, G., *et al. Doping Graphene with Metal Contacts* Phys. Rev. Lett.101, 026803 (2008).

[149] Wang, B., *et al., Chemical origin of a graphene moiré overlayer on Ru(0001).* Phys. Chem. Chem. Phys. 10, 3530 (2008).

[150] Morits, W., *et al., Structure Determination of the Coincidence Phase of Graphene on Ru(0001)* Phys. Rev. Lett. 104, 136102 (2010).

[151] Borca, B., *et al., Electronic and geometric corrugation of periodically rippled, self-nanostructured graphene epitaxially grown on Ru(0001)* New J. Phys. 12, 093018 (2010).

[152] Vanin, M., *et al., Graphene on metals: A van der Waals density functional study.* Phys. Rev. B 81, 081408(R) (2010).

[153] Stradi, D., *et al., Role of Dispersion Forces in the Structure of Graphene Monolayers on Ru Surfaces.* Phys. Rev. Lett. 106, 186102 (2011).

[154] Ugeda, M. M., *et al., Missing Atom as a Source of Carbon Magnetism.* Phys. Rev. Lett. 104, 096804 (2010).

[155] N'Diaye, A. T., *et al., In situ observation of stress relaxation in epitaxial graphene*. New J. Phys. 11, 113056 (2009)

[156] Rusponi, S., *et al., Highly Anisotropic Dirac Cones in Epitaxial Graphene Modulated by an Island Superlattice.* Phys. Rev. Lett. 105, 246803 (2010)

[157] Gyamfi, M., *et al., Inhomogeneous electronic properties of monolayer graphene on Ru(0001)* Phys. Rev. B 83, 153418 (2011)

[158] Pletikosić, I., *et al., Dirac Cones and Minigaps for Graphene on Ir(111)* Phys. Rev. Lett. 102, 056808 (2009).

[159] Varykhalov, A., *et al., Electronic and Magnetic Properties of Quasifreestanding Graphene on Ni.* Phys. Rev. Lett. 101, 157601 (2008).

[160] Balog, R., *et al., Bandgap opening in graphene induced by patterned hydrogen adsorption.* Nature Mater. 9, 315 (2010).

[161] Haberer, D., *et al., Tunable Band Gap in Hydrogenated Quasi-Free-Standing Graphene.* Nano Lett. 10, 3360 (2010).

[162] Rader, O., *et al., Is There a Rashba Effect in Graphene on 3d Ferromagnets?* Phys. Rev. Lett. 102, 057602 (2009).

[163] N'Diaye, A. T., *et al., A versatile fabrication method for cluster Superlattices.* New J. Phys. 11, 103045 (2009).

[164] Pozzo, M., *et al., Thermal Expansion of Supported and Freestanding Graphene: Lattice Constant versus Interatomic Distance* Phys. Rev. Lett. 106, 135501 (2011).

[165] Sun, Z., *et al., Topographic and electronic contrast of the graphene moiré on Ir(111) probed by scanning tunneling microscopy and noncontact atomic force microscopy* Phys. Rev. B 83, 081415(R) (2011).

[166] Altenburg, S. J. , *et al., Graphene on Ru(0001): Contact Formation and Chemical Reactivity on the Atomic Scale* Phys. Rev. Lett. 105, 236101 (2010).

[167] Hill, E.W., *et al., Graphene Spin Valve Devices.* IEEE TRANSACTIONS ON MAGNETICS, VOL. 42, 2694 (2006).

[168] Weser, M., *et al., Electronic structure and magnetic properties of the graphene/Fe/Ni(111) intercalation-like system* Phys. Chem. Chem. Phys. 13, 7534 (2011).

[169] Vo-Van, C., *et al., Ultrathin epitaxial cobalt films on graphene for spintronic investigations and applications* New J. Phys. 12, 103040 (2010).

[170] Yazyev, O. V., Pasquarello, A., *Magnetoresistive junctions based on epitaxial graphene and hexagonal boron nitride.* Phys. Rev. B 80, 035408 (2009).

[171] Sicot, M., *et al., Nucleation and growth of nickel nanoclusters on graphene Moiré on Rh(111)* Appl. Phys. Lett. 96, 093115 (2010).

[172] Donner, K. , Jakob, P., *Structural properties and site specific interactions of Pt with the graphene/Ru(0001) moiré overlayer.* J. Chem. Phys. 131, 164701 (2010).

[173] Pollard, A. J., *et al., Supramolecular Assemblies Formed on an Epitaxial Graphene Superstructure.* Angew. Chem. Int. Ed. 49, 1794 (2010).

[174] Tontegode, A. Y. *, Carbon on transition metal surfaces* Prog. Surf. Sci. 38, 201 (1991).

[175] Coraux, J., *et al., Growth of graphene on Ir(111)* New J. Phys. 11, 023006 (2009).

[176] Gao, M., et al., *Tunable interfacial properties of epitaxial graphene on metal substrates* Appl. Phys. Lett. 96, 053109 (2010).

[177] van Gastel, R., *et al., Selecting a single orientation for millimeter sized graphene sheets.* Appl. Phys. Lett. 95, 121901 (2009).

[178] Günther, S., *et al., Single Terrace Growth of Graphene on a Metal Surface.* Nano Lett. 11, 1895 (2011).

[179] Hattab, H., *et al., Growth temperature dependent graphene alignment on Ir(111)* Appl. Phys. Lett. 98, 141903 (2011).

[180] Dong, G. et al. (in press)

[181] Iwasaki, T., *et al., Long-Range Ordered Single-Crystal Graphene on High-Quality Heteroepitaxial Ni Thin Films Grown on MgO(111).* Nano Lett. 11, 79 (2011)

[182] Vo-Van, C., *et al., Epitaxial graphene prepared by chemical vapor deposition on single crystal thin iridium films on sapphire* Appl. Phys. Lett. 98, 181903 (2011).

[183] Park, H. J., *et al., Growth and properties of few-layer graphene prepared by chemical vapor deposition.* Carbon 48, 1088 (2009).

[184] Amara, H., Bichara, C. , Ducastelle, F., *Formation of carbon nanostructures on nickel surfaces: A tight-binding grand canonical Monte Carlo study.* Phys. Rev. B 73, 113404 (2006).

[185] Amara H., *et al., Tight-binding potential for atomistic simulations of carbon interacting with transition metals: Application to the Ni-C system.* Phys. Rev. B 79, 014109 (2009).

[186] Karoui, S., *et al., Nickel-Assisted Healing of Defective Graphene.*
ACS Nano 4, 6114 (2010).

[187] Thiel, S., *et al., Engineering polycrystalline Ni films to improve thickness uniformity of the chemical-vapor-deposition-grown graphene films.* Nanotechnology 21, 015601 (2010).

[188] Baraton, L. et al., Europhys. Lett., in press

[189] Dervishi, E., *et al., The role of hydrocarbon concentration on the synthesis of large area few to multi-layer graphene structures.* Chem. Phys. Lett. 501, 390 (2011).

[190] Hesjelda, T., *Continuous roll-to-roll growth of graphene films by chemical vapor deposition.* Appl. Phys. Lett. 98, 133106 (2011).

[191] Mattevi, C., Kim, H., Chhowalla, M., *A review of chemical vapour deposition of graphene on copper.* J. Mater. Chem. 21, 3324 (2011).

[192] Oznuler, T., *et al., Synthesis of graphene on gold*. Appl. Phys. Lett. 98, 183101 (2011).

[193] Robertson, A. W., Warner, J. H., *Hexagonal Single Crystal Domains of Few-Layer Graphene on Copper Foils.* Nano Lett. 11, 1182 (2011).

[194] Wu, Y. A., *et al., Aligned Rectangular Few-Layer Graphene Domains on Copper Surfaces. Chem. Mater.* 23, 4544 (2011).

[195] Lherbier, A., *et al., Charge Transport in Chemically Doped 2D Graphene.* Phys. Rev. Lett. 101, 036808 (2008).

[196] Bieri, M., et. al. *Porous graphenes: two-dimensional polymer synthesis with atomic precision.* Chem Commun. 2009 , 6919-6921.

[197] Booth, T., *et al, Discrete Dynamics of Nanoparticle Channelling in Suspended Graphene.* Nano Lett. 11, 2689 (2011).

[198] Tapaszto, L., *et al., Tailoring the atomic structure of graphene nanoribbons by scanning tunnelling microscope lithography.* Nature Nanotech. 3, 397-401 (2008).

[199] Wagner, P., Bezanilla, A., Roche, S., Ivanovskaya, V. V., Rayson, M. J., Ewels, C. P. in preparation (2011)

[200] Cervantes-Sodi, F., *et al., Edge-functionalized and substitutionally doped graphene nanoribbons: Electronic and spin properties.* Phys. Rev. B. 77, 165427 (2008).

[201] Ivanovskaya, V. V., *et al, Low-energy termination of graphene edges via the formation of narrow nanotubes.* Phys. Rev. Lett., 107, 065502 (2011).

[202] Wagner, P., *et al, Ripple edge engineering of graphene nanoribbons*. arXiv:1107.1977v1 (2011).

[203] Cocchi, C., et al., *Designing All-Graphene Nanojunctions by Covalent Functionalization*J. Phys. Chem. C, 115, 2969 (2011).

[204] Biel, B., *et al., Anomalous Doping Effects on Charge Transport in Graphene Nanoribbons.* Phys. Rev. Lett. 102, 096803 (2009).

[205] Banhart, F., Kotakoski, J. Krasheninnikov, A. V., *Structural Defects in Graphene*. ACS Nano 5, 26 (2011).

[206] Ferrari, A. C. and Robertson, J. (eds), Raman spectroscopy in carbons: from nanotubes to diamond, Theme Issue, Phil. Trans. Roy. Soc. A 362, 2267-2565 (2004).

[207] Nemanich, R.J., Solin, S. A., Martin, R.M., *Light-scattering study of boron nitride microcrystals*, Phys. Rev. B 23, 6348 (1981).

[208] Reich, S., *et al., Resonant Raman scattering in cubic and hexagonal boron nitride*. Phys. Rev B 71, 205201 (2005).

[209] Russo V. *et al. Raman spectroscopy of Bi-Te thin films.* J. Raman Spectrosc. 39, 205 (2008)

[210] Gordon, R. J., *Criteria for Choosing Transparent Conductors*. MRS Bulletin 8, 53 (2000).

[211] Hamberg, I. and Granqvist, C. G., *Evaporated Sn-doped In_2O_3 films: basic optical properties and applications to energy-efficient windows*. J. Appl. Phys. 60, R123 (1986).

[212] Granqvist, C. G., *Transparent conductors as solar energy materials: a panoramic review.* Sol. Energy Mater. Sol. Cells 91, 1529–1598 (2007).

[213] Sheraw, C. D., *et al., Organic thin-fi lm transistor-driven polymer dispersed liquid crystal displays on fl exible polymeric substrates.* Appl. Phys. Lett. 80, 1088 (2002).

[214] Lee, J. Y., et al., *Solution-processed metal nanowire mesh transparent electrodes.* Nano Lett. 8, 689 (2008).

[215] De, S., *et al. Silver nanowire networks as fl exible, transparent, conducting films: extremely high dc to optical conductivity ratios*. ACS Nano 3, 1767 (2009).

[216] Geng, H. Z., *et al., Effect of acid treatment on carbon nanotube-based flexible transparent conducting films.* J. Am. Chem. Soc. 129, 7758 (2007).

[217] Wu, Z., *et al., Transparent, conductive carbon nanotube films.* Science 305, 1273 (2004).

[218] De, S. and Coleman, J. N,. *Are there fundamental limitations on the sheet resistanceand transmittance of thin graphene films?* ACS Nano 4, 2713 (2010).

[219] Casiraghi, C., et al., *Raman fingerprint of charged impurities in graphene* Appl. Phys. Lett. 91, 233108 (2007)

[220] Sahu, D. R., Lin, S. Y. and Huang, J. L., *ZnO/Ag/ZnO multilayer films for the application of a very low resistance transparent electrode*. Appl. Surf. Sci. 252, 7509 (2006).

[221] Zhu, Y., *et al., Rational Design of Hybrid Graphene Films for High-Performance Transparent Electrodes.* Acs Nano 5, 6472 (2011).

[222] Wang, X., Zhi, L., and Mullen, K., *Transparent, conductive graphene electrodes for dye-sensitized solar cells.* Nano Lett. 8, 323 (2007).

[223] Eda, G., Fanchini, G. & Chhowalla, M., *Large-area ultrathin films of reduced graphene oxide as a transparent and flexible electronic material.* Nature Nanotech. 3, 270 (2008).

[224] King, P. J., *et al.,Improvement of Transparent Conducting Nanotube Films by Addition of Small Quantities of Graphene*. ACS Nano 4, 4238 (2010).

[225] Matyba, P., *et al., Graphene and mobile ions: the key to all-plastic, solution processed light-emitting devices*. ACS Nano 4, 637 (2010).

[226] Bonaccorso, F., *Graphene photonics and optoelectronic*. ArXiv1006.4854v1.

[227] Tung, V. C., *et al,. Low-temperature solution processing of graphene-carbon nanotube hybrid materials for high-performance transparent conductors.* Nano Lett. 9, 1949 (2009).

[228] Chapin, D. M., Fuller, C. S. and Pearson, G. L., *A new silicon p-n junction photocell for converting solar radiation into electrical power.* J. Appl. Phys. 25, 676 (1954).

[229] Green, M. A., *et al., Solar cell efficiency tables*. Prog. Photovolt. Res. Appl. 7, 321 (1999).

[230] Peter, L. M., *Towards sustainable photovoltaics: the search for new material.* Phil. Trans. R. Soc. A 369, 1840 (2011).

[231] Li, X., *et al., Graphene-On-Silicon Schottky Junction Solar Cells.* Adv. Mater. 22, 2743,(2010).

[232] Wang, X., et al., *Transparent carbon films as electrodes in organic solar cells*. Angew. Chem. 47, 2990 (2008).

[233] De Arco, L. G., *et al., Continuous, highly flexible, and transparent graphene films by chemical vapor deposition for organic photovoltaics*" ACS Nano 4, 2865 (2010).

[234] Liu, Z., *et al.*, *Organic photovoltaic devices based on a novel acceptor material: Graphene*. Adv. Mater. 20, 3924 (2008).

[235] Yong, Y., Tour, J. M., *Theoretical efficiency of nanostructured graphene-based photovoltaics.* Small 6, 313 (2009).

[236] Yang, N., *et al., Two-dimensional graphene bridges enhanced photoinduced charge transport in dye-sensitized solar cells* ACS Nano 4, 887 (2010).

[237] Yan, X., *et al.*, "*Large, Solution-Processable Graphene Quantum Dots as Light Absorbers for Photovoltaics*" Nano Lett., 10, 1869, (2010).

[238] Stoller, M. D., *et al*., *Graphene-based ultracapacitor*. Nano Lett., vol. 8, 3498 (2008).

[239] Hong, W., *et al.*, *Transparent graphene/PEDOT-PSS composite fi lms as counter electrodes of dye sensitized solar cells*" Electrochem. Commun. 10, 1555 (2008).

[240] Bonaccorso, F., *et al., Graphene-based Natural Dye-Sensitized Solar Cells" Graphene 2011, Imaginenano 11-14 April, Bilbao, (Spain).*

[241] Echtermeyer, T.J., *et al. Strong plasmonic enhancement of photovoltage in graphene*. Nature Comm. 2, 458 (2011).

[242] Burroughes, J. H., *et al. Light-emitting diodes based on conjugated polymers*. Nature 347, 539–541 (1990).

[243] Wu, J., *et al. Organic light-emitting diodes on solution-processed graphene transparent electrodes*. ACS Nano 4, 43–48 (2009).

[244] Han, T-H., *et al., Extremely efficient flexible organic light emitting diodes with modified graphene anode.* Nature Photon. 6, 105 (2012).

[245] Pickering, J. A., *Touch-sensitive screens: the technologies and their applications.* Int. J. Man. Mach. Stud. 25, 249 (1986).

[246] Silfverberg, M. 5th International Symposium, Mobile HCI 2003, Udine, Italy, 2003.

[247] Beecher, P., *et al., Material Choices For Haptic Interfaces*. Material Research Society 2011 Spring Meeting April 26-29, 2011 San Francisco, California (USA).

[248] E. Mallinckrodt, A. L. Hughes, W., Sleator Science, 118, 277 (1953)

[249] Kaczmarek, K. A. *et al., Polarity Effect in Electrovibration for Tactile Display," Biomedical Engineering*. IEEE Transactions on, 53, 2047 (2006).

[250] Saleh, B. E. A. & Teich, M. C. Fundamentals of Photonics Ch. 18, 784–803 (Wiley, 2007).

[251] Dawlaty, J. M., *et al. Measurement of the optical absorption spectra of epitaxial graphene from terahertz to visible*. Appl. Phys. Lett. 93, 131905 (2008).

[252] Wright, A. R., Cao, J. C. and Zhang, C., *Enhanced optical conductivity of bilayer graphene nanoribbons in the terahertz regime.* Phys. Rev. Lett. 103, 207401 (2009).

[253] Sun, Z., *et al. Graphene mode-locked ultrafast laser*. ACS Nano 4, 803–810 (2010).

[254] Mueller, T., Xia, F. and Avouris, P., *Graphene photodetectors for high-speed optical communications*. Nature Photon. 4, 297 (2010).

[255] Vasko, F. T., and Ryzhii, V., *Photoconductivity of intrinsic graphene*. Phys. Rev. B 77, 195433 (2008).

[256] Park, J., Ahn, Y. H. and Ruiz-Vargas, C., *Imaging of photocurrent generation and collection in single-layer graphene*. Nano Lett. 9, 1742 (2009).

[257] Xia, F. N., *et al. Photocurrent imaging and effi cient photon detection in a graphene transistor*. Nano Lett. 9, 1039 (2009).

[258] Xia, F., et al., *Ultrafast graphene photodetector*. Nature Nanotech. 4, 839 (2009).

[259] Xu, X. D., *et al., Photo-thermoelectric eff ect at a graphene interface junction*. Nano Lett. 10, 562 (2010).

[260] Gabor, N. M., *et al., Hot Carrier–Assisted Intrinsic Photoresponse in Graphene.* Science 334, 648 (2011)

[261] Blake, P., *et al. Influence of metal contacts and charge inhomogeneity on transport properties of graphene near the neutrality point.* Solid State Commun.149, 1068 (2009)

[262] Kang, Y. M. , *et al. Monolithic germanium/silicon avalanche photodiodes with 340 GHz gain–bandwidth product.* Nature Photon. 3, 59 (2009)

[263] Kuzmenko, A. B., et al., *Universal optical conductance of graphite*. Phys. Rev. Lett. 100, 117401 (2008).

[264] Lee, E. J. H., et al. Contact and edge effects in graphene devices. Nat. Nanotechnol. 3, 486 (2008)

[265] Konstantatos, G., *et al., Hybrid graphene-quantum dot phototransistors with ultrahigh gain*. ArXiv. 1112.4730v1

[266] Engel, M., *et al.,Light-matter interaction in a microcavity-controlled graphene transistor*. arXiv:1112.1380v1.

[267] Vahala, K. J., *Optical microcavities*. Nature 424, 839 (2003).

[268] Freitag, M., *et al., Thermal infrared emission from biased graphene*. Nat. Nanotechnol. 5, 497 (2010).

[269] Berciaud, S., *et al., Electron and Optical Phonon Temperatures in Electrically Biased Graphene*. Phys. Rev. Lett. 104, 227401 (2010).

[270] Keller, U., *Recent developments in compact ultrafast lasers.* Nature 424, 831 (2003).

[271] Okhotnikov, O., Grudinin, A., Pessa, M., *Ultra-fast fibre laser systems based on SESAM technology: new horizons and applications.* New J. Phys. 6, 177 (2004)

[272] Hasan, T., *et al. Nanotube–polymer composites for ultrafast photonics.* Adv. Mater. 21, 3874 (2009).

[273] Breusing, M., Ropers, C. and Elsaesser, T., *Ultrafast carrier dynamics in graphite.* Phys. Rev. Lett. 102, 086809 (2009).

[274] Sun, D., *et al., Ultrafast Relaxation of Excited Dirac Fermions in Epitaxial Graphene Using Optical Differential Transmission Spectroscopy.* Phys. Rev. Lett. 101, 157402, (2008).

[275] Sun, Z., *et al., High-power ultrafast solid-state laser using graphene based saturable absorber,* in The Conference on Lasers and Electro-Optics(Baltimore, US, 2011), JWA79.

[276] Popa, D., *et al., Sub 200fs pulse generation from a graphene mode-locked fiber laser.* Appl. Phys. Lett. 97, 203106 (2010)

[277] Popa, D., et al., *Graphene Q-switched, tunable fiber laser".* Appl. Phys. Lett. 98, 073106 (2011)

[278] Popa, D., et al., *Sub 200fs pulse generation from a graphene mode-loched fiber laser.* Appl. Phys. Lett. 97, 203106 (2010).

[279] Zhang, H., *et al. Vector dissipative solitons in graphene mode locked fiber lasers.* Opt. Commun. 283, 3334 (2010).

[280] Zhang, H., *et al. Compact graphene mode-locked wavelength-tunable erbium-doped fiber lasers: from all anomalous dispersion to all normal dispersion*. Laser Phys. Lett. 7, 591 (2010).

[281] Yu, H., *et al. Large Energy Pulse Generation Modulated by Graphene Epitaxially Grown on Silicon Carbide*. ACS Nano 4, 7582 (2010).

[282] Chang, Y. M.,et al., *Multilayered graphene efficiently formed by mechanical exfoliation for non linear saturable absorbers in fiber mode locked lasers.* Appl. Phys. Lett. 97, 211102 (2010).

[283] Martinez, A., Fuse, K. and Yamashita, S., *Mechanical exfoliation of graphene for the passive mode-locking of fiber lasers.* 99, 121107 (2011).

[284] Tan, W. D., et al., *Mode locking of ceramic Nd:yttrium aluminum garnet with graphene as a saturable absorber.* Appl. Phys. Lett. 96, 031106 (2010).

[285] Cho, W. B. et al., *High-quality, large-area monolayer graphene for efficient bulk laser mode-locking near 1.25 um*. Opt. Lett., 36, 4089-4091 (2011)

[286] Martinez, A., et al., *Optical deposition of graphene and carbon nanotubes in a fiber ferrule for passive mode-locked lasing*. Opt. Express 18, 23054 (2010).

[287] Wang, F. ,et al., *~2um Graphene Q-switched Thulium Fiber Laser*. Submitted (2011).

[288] Sun, Z., *et al., A stable, wideband tunable, near transform-limited, graphene-mode-locked, ultrafast laser.* Nano Res. 3, 404 (2010).

[289] W. Koechner, Solid-State Laser Engineering (Springer, New York, 2006).

[290] Lee, C.-C. et al., *Ultra-Short Optical Pulse Generation with Single-Layer Graphene.* J. Nonlinear Opt. Phys. Mater. 19, 767-771 (2010).

[291] Bass, M., Li, G. and Stryland, E. V. Handbook of Optics IV (McGraw-Hill, 2001).

[292] Wang, J. *et al., Broadband nonlinear optical response of graphene dispersions.* Adv. Mater. 21, 2430 (2009).

[293] Xu, Y., *et al. A graphene hybrid material covalently functionalized with porphyrin: synthesis and optical limiting property*. Adv. Mater. 21, 1275 (2009).

[294] Mikhailov, S. A. *Non-linear electromagnetic response of graphene.* Europhys. Lett. 79, 27002 (2007).

[295] Dean, J. J. and van Driel, H. M., *Second harmonic generation from graphene and graphitic films*. Appl. Phys. Lett. 95, 261910 (2009).

[296] Hendry, E., et al., *Strong nonlinear optical response of graphene flakes measured by four-wave mixing.* Phys. Rev. Lett. 105, 097401 (2010).

[297] Dhar, S. *et al., A new route to graphene layers by selective laser ablation* AIP ADVANCES 1, 022109 (2011).

[298] ITRS roadmap 2009, www.itrs.net (2011).

[299] Lemme, M.C., *et al., Towards Graphene Field Effect Transistors.* ECS Transactions, 11, 413 (2007).

[300] Lemme, M.C., *et al., A Graphene Field-Effect Device.* Electron Device Letters, IEEE, 28, 282 (2007).

[301] Echtermeyer, T. J., *et al., Graphene field-effect devices.* European Physical Journal-Special Topics. 148, 19 (2007)

[302] Williams, J.R., Di Carlo, L. and Marcus, C.M., *Quantum Hall Effect in a Gate-Controlled p-n Junction of Graphene.* Science 317, 638 (2007).

[303] Takagi, S., *et al., On the universality of inversion layer mobility in Si MOSFET's: Part I-effects of substrate impurity concentration.* Electron Devices, IEEE Transactions 41, 2357 (1994).

[304] Martin, J., *et al., Observation of electron-hole puddles in graphene using a scanning single-electron transistor*. Nature Phys. 4, 144 (2008).

[305] Lemme, M.C., *et al., Mobility in graphene double gate field effect transistors.* Solid-State Electronic 52, 514 (2008).

[306] Lin, Y.-M., *et al., Operation of Graphene Transistors at Gigahertz Frequencies.* Nano Lett. 9, 422 (2009).

[307] Nakada, K., et al., Edge state in graphene ribbons: Nanometer size effect and edge shape dependence. Physical Review B. 54, 17954 (1996).

[308] Barone, V., Hod, O., and Scuseria G.E., Electronic Structure and Stability of Semiconducting Graphene Nanoribbons. Nano Lett. 6, 2748 (2006).

[309] Son, Y.-W., Cohen, M.L. and Louie S.G., *Energy Gaps in Graphene Nanoribbons*. Phys. Rev. Lett. 97, 216803 (2006).

[310] Obradovic, B., *et al., Analysis of graphene nanoribbons as a channel material for field-effect transistors*. Appl. Phys. Lett. 88, 142102 (2006).

[311] Yang, L., et al., *Band-gap change of carbon nanotubes: Effect of small uniaxial and torsional strain.* Phys. Rev. B, 60, 13874 (1999).

[312] Fujita, M., *et al., Peculiar Localized State at Zigzag Graphite Edge*. J. Phys. Soc. Jpn. 65, 1920 (1996).

[313] Huang, B*., et al., Making a field effect transistor on a single graphene nanoribbon by selective doping*. Appl. Phys. Lett.. 91, 253122 (2007).

[314] Yan, Q., *et al., Intrinsic Current-Voltage Characteristics of Graphene Nanoribbon Transistors and Effect of Edge Doping*. Nano Lett. 7, 1469 (2007).

[315] Kan, E.-J., *et al., Will zigzag graphene nanoribbon turn to half metal under electric field?* Appl. Phys. Lett. 91, 243116 (2007).

[316] Hod, O., *et al., Enhanced Half-Metallicity in Edge-Oxidized Zigzag Graphene Nanoribbons*. Nano Lett. 7, 2295 (2007).

[317] Kudin, K.N., *Zigzag Graphene Nanoribbons with Saturated Edges*. ACS Nano 2, 516 (2008).

[318] Yoon, Y. and Guo, J. *Effect of edge roughness in graphene nanoribbon transistors*. Appl. Phys. Lett. 91, 073103 (2007).

[319] Sols, F., Guinea, F. and Neto A.H.C., *Coulomb Blockade in Graphene Nanoribbons*. Phys. Rev. Lett. 99, 166803 (2007).

[320] Cervantes-Sodi, F., *et al., Edge-functionalized and substitutionally doped graphene nanoribbons: Electronic and spin properties*. Phys. Rev. B 77, 165427 (2008).

[321] Han, M.Y., *et al., Energy Band-Gap Engineering of* Graphene Nanoribbons. Phys. Rev. Lett. 98 206805 (2007).

[322] Chen, Z., *et al., Graphene nano-ribbon electronics.* Physica E: Low-dimensional Systems and Nanostructures 40, 228 (2007).

[323] Han, M.Y., *et al., Electron Transport in Disordered Graphene Nanoribbons* Phys. Rev. Lett.104, 056801 (2010).

[324] Ponomarenko, L.A., *et al., Chaotic Dirac Billiard in Graphene Quantum Dots.* Science 320, 356 (2008).

[325] Wang, X., *et al., Room-Temperature All-Semiconducting Sub-10-nm Graphene Nanoribbon Field-Effect Transistors*. Phys. Rev. Lett. 100, 206803 (2008).

[326] Lemme, M.C., *et al., Etching of Graphene Devices with a Helium Ion Beam*. ACS Nano, 3, 2674 (2009).

[327] Bell, D.C., *et al., Precision Cutting and Patterning of Graphene with He Ions.* Nanotechnology 20, 455301 (2009).

[328] McCann, E., *Asymmetry gap in the electronic band structure of bilayer graphene.* Physical Review B (Condensed Matter and Materials Physics) 74, 161403 (2006).

[329] Ohta, T., et al., *Controlling the Electronic Structure of Bilayer Graphene.* Science 313, 951 (2006).

[330] Mak K. F., et al., *Observation of an Electric-Field-Induced Band Gap in Bilayer Graphene by Infrared Spectroscopy* Phys. Rev. Lett. 102, 256405 (2009).

[331] Zhang, Y. T. *et al., Direct observation of a widely tunable bandgap in bilayer graphene.* Nature 459, 820 (2009).

[332] Oostinga, J.B., et al., *Gate-induced insulating state in bilayer graphene devices.* Nature Mater. 7, 151 (2008).

[333] Szafranek, B. N. *et al., Electrical observation of a tunable band gap in bilayer graphene nanoribbons at room temperature* Appl. Phys. Lett. 96, 112103 (2010).

[334] Szafranek, B. N. *et al., High On/Off Ratios in Bilayer Graphene Field Effect Transistors Realized by Surface Dopants.* Nano Lett. 11, 2640 (2011).

[335] Li, S-L., et al., *Complementary-like Graphene Logic Gates Controlled by Electrostatic Doping.* Small 7, 1552 (2011).

[336] Schwierz, F. and Liou, J.J., *RF transistors: Recent developments and roadmap toward terahertz applications.* Solid-State Electronics. 51, 1079 (2007).

[337] Frank, D.J., Taur, Y. and Wong, H.S.P., *Generalized scale length for two-dimensional effects in MOSFETs.* Electron Device Letters, IEEE. 19, 385 (1998).

[338] Meric, I., *et al. RF performance of top-gated, zero-bandgap graphene field-effect transistors*. in Electron Devices Meeting, 2008. IEDM 2008. IEEE International. 2008.

[339] Moon, J.S., et al., Epitaxial-Graphene RF Field-Effect Transistors on Si-Face 6H-SiC Substrates. Electron Device Letters, IEEE. 30, 650 (2009).

[340] Palacios, T., Hsu, A., and Wang H. *Applications of graphene devices in RF* communications. Communications Magazine, IEEE 48, 122 (2010).

[341] Lin, Y-M., *et al., 100-GHz Transistors from Wafer-Scale Epitaxial Graphene*. Science 327, 662 (2010).

[342] Schwierz, F. and Liou, J. J. *Modern Microwave Transistors – Theory, Design, and Performance* (Wiley, 2003).

[343] Wu, Y., et al., *High-frequency, scaled graphene transistors on diamond-like carbon*, Nature 472, 74 (2011).

[344] Liao, L., *et al.High-speed graphene transistors with a self-aligned nanowire gate.* Nature 467, 305 (2010).

[345] Schwierz, F., Graphene transistors. Nature Nanotech. 5, 487 (2010)

[346] http://www.itrs.net/Links/2010ITRS/IRC-ITRS-MtM-v2%203.pdf

[347] Wu, X., *et al., Epitaxial-Graphene/Graphene-Oxide Junction: An Essential Step towards Epitaxial Graphene Electronics.* Phys. Rev. Lett. 101, 026801 (2008).

[348] Standley, B., et al., Graphene-Based Atomic-Scale Switches. Nano Letters, 2008. 8(10): p. 3345-3349.

[349] Boukhvalov, D.W. and Katsnelson, M.I. , *Tuning the gap in bilayer graphene using chemical functionalization: Density functional calculations*. Phys. Rev. B 78, 085413 (2008).

[350] Echtermeyer, T.J., *et al., Nonvolatile Switching in Graphene Field-Effect Devices*. Electron Device Letters, IEEE. 29, 952 (2008).

[351] Zheng, Y., *et al., Gate-controlled nonvolatile graphene-ferroelectric memory*. Appl. Phys. Lett. 94, 163505 (2009).

[352] Fiori, G., Iannaccone, G., *On the possibility of tunable-gap bilayer graphene FET*, IEEE Electron Device Letters, Vol. 30, pp. 261-264, 2009.

[353] Fiori, G., Iannaccone, G., *Ultralow-Voltage Bilayer graphene tunnel FET*, IEEE Electron Device Letters, Vol. 30, pp.1096-1098, 2009.

[354] Chang, L., *et al., Extremely Scaled Silicon Nano-CMOS Device*. Proceedings of the IEEE, 91, 1860 (2003).

[355] Hu, C., *et al., Green Transistor - A VDD Scaling Path for Future Low Power ICs*. IEEE VLSI Technology, Systems and Applications, 2008. VLSI-TSA 2008.

[356] Britnell, L., *et al., Field-effect tunneling transistor based on vertical graphene heterostructures*. ArXiv1112.4999.

[357] Geim, A.K., *QED in a Pencil Trace* KITP Graphene Workshop 01-09-07.

[358] Fiori, G., Iannaccone, G. *Simulation of Graphene Nanoribbon Field-Effect Transistors*. IEEE, Electron Device Letters 28, 760 (2007).

[359] Yoon, Y., *et al., Performance Comparison of Graphene Nanoribbon FETs With Schottky Contacts and Doped Reservoirs*. IEEE Transaction on Electron Devices 55, 2314 (2008).

[360] Grassi, R., *et al., Hierarchical modeling of carbon nanoribbon devices for CNR-FETs engineering*, Device Research Conference, 2008.

[361] Betti, A., Fiori, G., Iannaccone, G., *Atomistic Investigation of Low-Field Mobility in Graphene Nanoribbons* ,IEEE Trans. Electr. Dev., available at: ieeexplore.ieee.org

[362] Ferry, D. K., Semiconductor transport London: Taylor & Francis, 2000. Technology & Engineering ISBN 0-7484-0865-7.

[363] Elias, D. , *et al., Control of Graphene's Properties by Reversible Hydrogenation: Evidence for Graphane*. Science 323, 610 (2009).

[364] Lebègue, S., *et al., Accurate electronic band gap of pure and functionalized graphane from GW calculations*. Phys. Rev. B 79, 245117 (2009).

[365] Fiori, G., *et al., Simulation of hydrogenated graphene field-effect transistors through a multiscale approach*. Phys. Rev. B, 82, 153404 (2010).

[366] Chauhan, J., and Guo, J., *Assessment of High-Frequency Performance Limits of Graphene Field-Effect Transistors*. Nano Res. 4, 571 (2011).

[367] Nam Do, V., *et al., Electronic transport and spin-polarization effects of relativisticlike particles in mesoscopic graphene structures*, J. Appl. Phys. 104, 063708 (2008).

[368] Hung Nguyen, V., *et al., Quantum transport of dirac fermions in graphene field effect transistors*, SISPAD 2010, p.9.

nanoresearch

Annex

Graphene vs carbon nanotube in electronic devices

Dr. Young Hee Lee

Center for Nanotubes and Nanostructured Composites, Sungkyunkwan Advanced Institute of Nanotechnology, Sungkyunkwan University, Suwon, 440-746, Korea
leeyoung@skku.edu

1. Transparent conducting films

In general carbon materials such as graphite and CNTs are black soots. Nevertheless, when the thickness of the film is far less than that of light wavelength, the light transmits mostly with a minimum absorbance. Highly flexible, transparent, and conducting films are one of the recent emerging technologies applied in flexible displays, electronic papers, and solar cells.

The monolayer graphene grown by chemical vapor deposition on copper substrate and transferred onto the polyethylene tere-phthalate (PET) substrate is shown in Figure 1a. The edge is clearly contrasted at the right side. The CNT film is also shown with similar transmittance in Figure 1b and 1c. The SEM image clearly shows surface morphology of CNT network (Figure 1c). The sheet resistance of the pristine CNT-TCF could be dramatically improved by chemical treatments. The doping effect on CNT-TCFsis presented in Figure 1d. The pristine SWCNT-TCF exhibits near about 360 Ω/sq sheet resistance at 90% transmittance. Afternitric acid treatment on the film removes the remaining surfactant from the CNT network and lowers the sheet resistance to 150 Ω/sq at 90% transmittance. Further doping by Au^{3+} ions reduces the sheet resistance to 110Ω/sq at 90% transmittance, which is the lowest value in the CNT film. On the other hand, monolayer graphene is transferred on the PET film layer-by-layer. With increasing the number of graphene layers, the transmittance and sheet resistance decrease and reaches 85% and 300Ω/sq respectively, at four layers.While each graphene layer is transferred, chemical doping with acid and Au^{3+} ions is also done similar to CNTs. The sheet resistances are consistently reduced at different layers. Interestingly, the sheet resistances of SWCNTs are similar to those of graphene in the transmittance range of 85~97%.

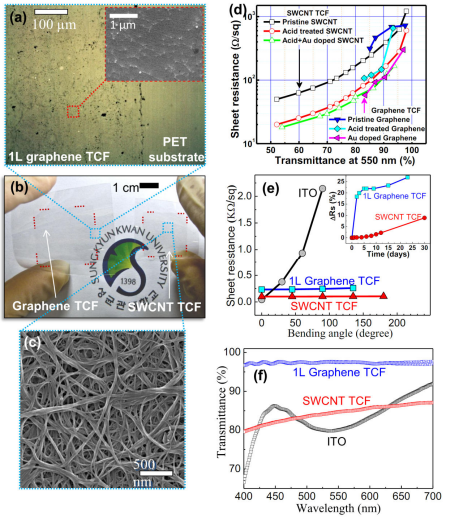

Fig. 1 > Graphene and carbon nanotube TCF devices: [1] (a) Microscopic image (optical) of a graphene TCF using PET substrate. Inset shows surface morphology (SEM micrograph) of the graphene TCF. (b) Digital image of the flexible, transparent graphene (left) and CNT (right) TCFs. (c) SEM micrograph of the CNT-TCF, representing the CNT network morphology in the film. (d) Comparisons of TCF characteristic curves between pristine, acid treated, and doped graphene and CNT TCFs. [2,3] (e) Sheet resistance variations with bending angle in graphene, SWCNT, ITO TCFs. Inset shows changes in sheet resistance ($\Delta Rs = [Rs_f - Rs_0]/ Rs_0 \times 100$, where Rs_0 is the sheet resistance value at zero time, and Rs_f is the final sheet resistance value at later time) variations with time in graphene, SWCNT FCTs. (f) Transmittance dependence on wavelengths in single layer graphene, SWCNT, and ITO transparent conducting films./

The advantage of nanocarbons is excellent flexibility, as shown in Figure 1e. While ITO shows a rapid increase in the sheet resistance due to cracking of the film as the bending angle increases, graphene and SWCNT film show almost no significant change in the sheet resistance. The inset shows environmental stability of both films. Although graphene reveals rather more sensitive change in the sheet resistance around 25%, the SWCNT film reveals much better stability up to less than 10% increase of the sheet resistance even after one month.Both graphene and CNT are highly flexible materials.For instance, monolayer graphene has a transmittance of nearly 97.5% (Figure 1f). Carbon nanotube film is also highly transparent at a thickness of less than 50 nm. The SWCNT TCF shows a gradual decrease of the transmittance with decreasing wavelength. On the other hand, Indium tin oxide shows strong spectral response.In particular, the transmittance drops rapidly near ultraviolet (UV) region, which is a serious drawback for UV sensors and LEDs even if the transmittance is very high in visible region. These facts highlight uniform transmittance of graphene and CNT TCFs with larger wavelength window than ITO films.

2. Doping strategy in graphene and carbon nanotubes

Although ambipolarity is an intrinsic property of graphene and CNT and can be utilized for switch operation, however, unipolar semiconducting materials are preferred in silicon technology. Doping is a traditional approach to control carrier type. The doping strategy for graphene and CNT is rather different. Although similar doping technique can be used during synthesis, formation energy of foreign atoms is rather large in carbon system.

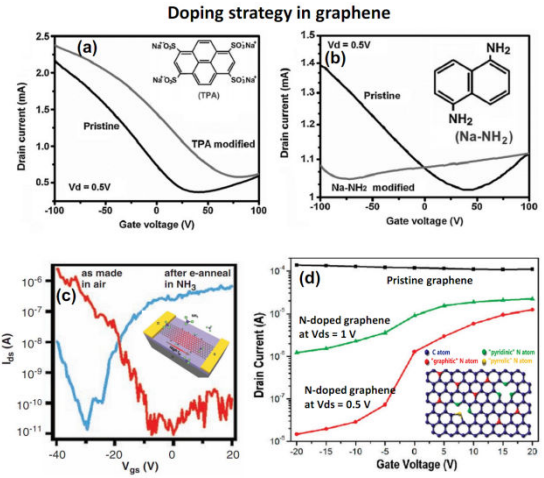

Fig. 2 > Doping strategy in graphene: (a) Transfer characteristics of a SLG-FET before and after TPA doping, figure inset is representing the chemical structure of TPA molecule.[4] (b) Transfer characteristics of a SLG-FET before and after Na-NH_2 doping, figure inset is representing the chemical structure of TPA molecule. [4] (c) Transfer curves of the as-made GNR-FET in vacuum (p-type, red) and after e-annealing in NH_3 (n-type, blue). [5] (d) Transfer characteristics of the pristine graphene (with V_{ds} = -0.5 V) and the N-doped graphene (V_{ds} at 0.5 and 1 V). Figure inset showing the schematic representation of the N-doped graphene [6]./

2.1. Doping strategy in graphene

Figure 2a and 2b represent doping of monolayer graphene using aromatic molecules. The transfer characteristics of the monolayer graphene FET shows p-type behavior intrinsically under ambient condition (Figure 2a). Threshold voltage in this case was observed at +30 V. However, tetrasodium1,3,6,8-pyrenetetrasulfonic acid (TPA) doped graphene transistor exhibits a higher source-drain current level at negative gate bias region with a threshold voltage of +80 V.

The increment in the threshold voltage from +30 V to +80 V indicates the TPA molecule induced hole (p-type) doping in graphene. Distinctly, graphene FET doped by Na-NH_2 molecules exhibits a lower current level in negative gate voltage region and slightly higher

current level in positive gate voltage regions (Figure 2b), shifting its threshold voltage from +28 V to -70 V. Electrical measurements on these graphene FET devices suggest that the aromatic molecules with electron withdrawing groups in TPA impose p-doping (lowering electron density) and electron donating groups (amine group) in Na-NH_2 cause n-doping (increasing electron density) in graphene. Similar n-type doping is also observed in GNR FET devices using NH_3 doping. Figure 2c shows the transfer characteristics of a 5nm width GNR FET device. Intrinsically device shows p-type characteristics under ambient conditions, ambipolar behavior after electrical annealing under vacuum (not shown here), and n-type behavior after electrical annealing under NH_3 gas atmosphere. After electrical annealing in NH_3, the GNR FET is converted to n-type, with on-current around 1 μA, and on/off ratio about 10^5, exhibiting good n-type characteristic. The transfer characteristics of the pristine p-type graphene in Figure 2d shows poor gate dependence and very low on/off ratio (top line). Significantly, nitrogen-doped graphene transform it into n-type with on/off ratio around 10^3 at 0.5 V source-drain voltage.

2.2. Chemical doping strategy of CNTs

Similar to graphene, various chemical doping strategies have been investigated to have n-type conversion and p-type enhancement behavior in CNTs under ambient conditions [2, 8-11]. The choice of chemical dopant is complicated by the fact that the redox potential of CNTs is strongly diameter-dependent [2]. Figure 3a shows redox potential of CNTs as a function of diameter and metallicity. Absolute redox potential reduces as the diameter increases. The Fermi levels of metallic and semiconducting CNTs also vary slightly with diameter. The *Vis* and *Cis* indicate the oxidation potential and reduction potential of the SWCNT from i^{th} energy level (van Hove singularity), respectively. The redox potentials of the chosen doping materials are also provided in the plot. For example, the Au^{3+} ion has the largest reduction potential of 1.50 V among others and is even larger than *V1s* and *V2s* of the semiconducting nanotubes independent of the diameter and the *V1m* of the metallic ones in large diameter region. This implies that Au^{3+} can be reduced by extracting electrons from both *V1s* and *V2s* for semiconducting CNTs and even *V1m* for metallic CNTs. Other dopant such as DDQ has smaller reduction potential (0.51 V)

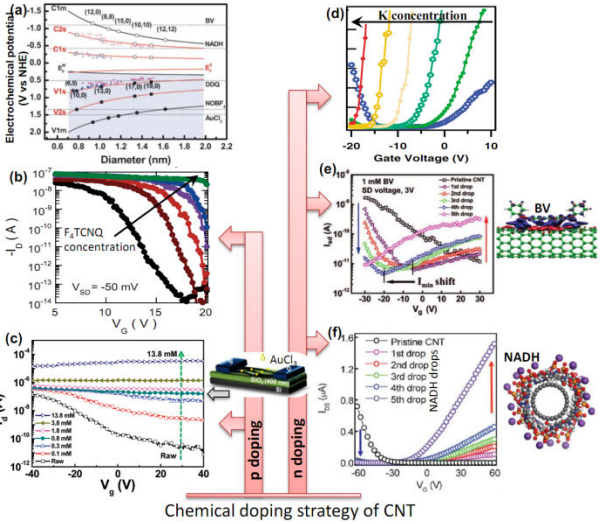

Fig. 3 > Chemical doping strategy of CNT: (a) Redox potential of various nanotubes as a function of the diameter. The values in parentheses indicate the chiral index of the SWCNTs. The reduction potentials of dopants are also provided as dotted lines. The triangle and reverse triangle indicate the experimental redox potentials of SWCNT. [2] (b) Logarithmic plot of change in transfer characteristics of the SWCNT-FET upon different concentrations of F_4TCNQ/solution. [7] (c) Transfer characteristics of a random network CNT-FET without and with p-type doping by $AuCl_3$ solution with a different solution concentrations. [8] (d) Transfer curve of the CNT-FET under different dose of potassium doping. [9] (e) Transfer characteristics of a CNT-FET, before and after n-type doping in terms of number of BV droplets. [10] (f) Transfer characteristics of a CNT-FET, before and after n-type doping in terms of number of NADH droplets [11]./

than Au^{3+}. In this case, DDQ can extract electrons from *V1s* of semiconducting CNTs with particularly large diameter region but no influence for metallic CNTs. The same logic is applied to the dopant with electron donating group. For instance, benzyl viologen (BV) has an oxidation potential of -1.1 V.[1] This implies that BV can donate electrons to the empty *C1s* and *C2s* of semiconducting CNTs and even to the empty *C1m* of metallic CNTs. Figure 3b shows the transfer characteristics of a CNT-FET using an increasing doping concentration of tetrafluorotetracyano-p-quinodimethane (F_4TCNQ). F_4TCNQ has a reduction potential in the range of 0.1 V to 0.2 V and therefore is an electron extractor and p-type dopant. Using increasing amount of F_4TCNQ dopant, the hole conductance of the device increases appreciably due to the increment of carrier concentration by doping. A drop of the F_4TCNQ solution causes a rigid shift in the transfer characteristics toward positive gate biasand the upshift of threshold voltage constitutes sufficient evidence for the precise control of carrier density in CNT-FETs. Similar hole conductance increment (p-type doping) in CNTs is also observed using $AuCl_3$ solution as a chemical dopant (Figure 3c). The transfer characteristics of CNT-FET in this case also shows gradual increment in hole conductance level with increasing hole carrier concentration. Figure 3d represents the transfer characteristics of potassium-doped CNT-FET with increasing doping concentrations. The pristine CNT-FET shows p-type behavior under ambient conditions. As potassium doping concentration increases (from right to left in the figure), CNT shows ambipolar behavior at low doping concentration and the threshold voltage is downshifted clearly, demonstrating n-type doping behavior.In another approach n-type conversion of CNTs is performed by benzyl viologen (BV) molecules. Figure 3e shows the transfer characteristics of CNT-FETs with different BV concentrations. With increasing BV concentrations, the hole current at the negative gate bias is suppressed, while the electron current is enhanced. Threshold voltage is down-shifted to the direction of the negative gate bias. This indicates a type conversion from the initial p-type to n-type in the CNT TFT. The right panel of the figure represents the isodensity surface plot of electron accumulation (red) and depletion (blue) due the adsorption of BV molecules on the CNT surface. Distinct type conversion of CNTs is also demonstrated by using *β*-Nicotinamide adenine dinucleotide (reduced dipotassium salt, NADH) as a dopant (Figure 3f). Here the pristine p-type CNT-FET under ambient conditionsshows a gradual conversion to n-type as the concentration of NADH molecules increases. The right panel of the figure represents the schematic of NADH adsorption on the CNT surface.

3. References

[1] Chandan Biswas, Young Hee Lee, Advanced Functional Materials, 2011, 21, 3806-3826.

[2] K. K. Kim, S.-M. Yoon, H. K. Park, H.-J.Shin, S. M. Kim, J. J. Bae, Y. Cui, J. M. Kim, J.-Y. Choi, Y. H. Lee, New J. Chem. 2010, 34, 2183-2183.

[3] F. Güneş, H. J. Shin, C. Biswas, G. H. Han, E. S. Kim, S. J. Chae, J.-Y. Choi, Y. H. Lee, ACS Nano 2010, 4, 4595-4600.

[4] X. Dong, D. Fu, W. Fang, Y. Shi, P. Chen, L. J. Li, Small 2009, 5, 1422-1426.

[5] X. Wang, X. Li, L. Zhang, Y. Yoon, P. K. Weber, H. Wang, J. Guo, H. Dai, Science 2009, 324, 768-771.

[6] D. Wei, Y. Liu, Y. Wang, H. Zhang, L. Huang, G. Yu, Nano Lett. 2009, 9, 1752-1758.

[7] T. Takenobu, T. Kanbara, N. Akima, T. Takahashi, M. Shiraishi, K. Tsukagoshi, H. Kataura, Y. Aoyagi, Y. Iwasa, Adv. Mater. 2005, 17, 2430-2434.

[8] I. H. Lee, U. J. Kim, H. B. Son, S. M. Yoon, F. Yao, W. J. Yu, D. L. Duong, J. Y. Choi, J. M. Kim, E. H. Lee, Y. H. Lee, J. Phys. Chem. C 2010, 114, 11618-11622.

[9] S. Heinze, J. Tersoff, R. Martel, V. Derycke, J. Appenzeller, P. Avouris, Phys. Rev. Lett. 2002, 89, 106801-106801.

[10] S. M. Kim, J. H. Jang, K. K. Kim, H. K. Park, J. J. Bae, W. J. Yu, I. H. Lee, G. Kim, D. D. Loc, U. J. Kim, E. H. Lee, H. J. Shin, J. Y. Choi, Y. H. Lee, J. Am. Chem. Soc. 2009, 131, 327-331.

[11] B. R. Kang, W. J. Yu, K. K. Kim, H. K. Park, S. M. Kim, Y. Park, G. Kim, H. J. Shin, U. J. Kim, E. H. Lee, J. Y. Choi, Y. H. Lee, Adv. Funct. Mater. 2009, 19, 2553-2559. *

nanoICT
Coordination Action

The nanoICT Coordination Action activities will reinforce and support the whole European Research Community in "ICT nanoscale devices" covering the following research areas expected to demonstrate unconventional solutions beyond the expected limits of CMOS technology:

1. Demonstration of new concepts for switches or memory cells
2. Demonstration of new concepts, technologies and architectures for local and chip level interconnects with substantial improvements over current solutions
3. Demonstration of radically new functionalities by the integration of blocks from a few nanometres down to the atomic scale into high added-value systems

The CA action plans will go beyond the organisation of conferences, workshops, exchange of personnel, WEB site, etc. developing the following activities:

* Consolidation and visibility of the research community in ICT nanoscale devices
* Mapping and benchmarking of research at European level, and its comparison with other continents
* Identification of drivers and measures to assess research in ICT nanoscale devices, and to assess the potential of results to be taken up in industrial research
* Coordination of research agendas and development of research roadmaps
* Coordination of national or regional research programmes or activities, with the aim to involve funding authorities in building the ERA around this topic
* Development of strategies for international cooperation on themes related to NanoICT

Expected impact will be the enhanced visibility, shaping and consolidation of the NanoICT research community in Europe.

Short Facts	
nanoICT	Nano-scale ICT Devices and Systems Instrument Coordination Action
EC contribution	1 M euros
Contract number	216165
Nº of partners	12
Coordinator	Phantoms Foundation (Spain) / Antonio Correia
Start date	January 01, 2008
Duration	36 months
WEB site	www.nanoict.org